NASA CR-54835
PWA-2796

FINAL REPORT
TURBINE RESEARCH PACKAGE FOR RESEARCH AND DEVELOPMENT OF HIGH PERFORMANCE TURBOALTERNATOR

written by

R. Cohen, W.K. Gilroy, F.D. Havens

approved by

P. Bolan

prepared for

NATIONAL AERONAUTICS AND SPACE ADMINISTRATION

CONTRACT NAS3-6013

Pratt & Whitney Aircraft DIVISION OF UNITED AIRCRAFT CORPORATION

EAST HARTFORD, CONNECTICUT

NASA CR-54885
PWA-2796

FINAL REPORT
TURBINE RESEARCH PACKAGE FOR RESEARCH AND DEVELOPMENT OF HIGH PERFORMANCE TURBOALTERNATOR

written by

R. Cohen, W. K. Gilroy, F. D. Havens

approved by

P. Bolan

prepared for

NATIONAL AERONAUTICS AND SPACE ADMINISTRATION

January 1967

CONTRACT NAS3-6013

Technical Management
NASA Lewis Research Center
Cleveland, Ohio
Space Power System Division
Henry B. Tryon
Fluid System Components Division
Consultant - Harold E. Rohlik

Pratt & Whitney Aircraft DIVISION OF UNITED AIRCRAFT CORPORATION

EAST HARTFORD • CONNECTICUT

COPY NO. 39

FOREWORD

This report was produced in accordance with NASA Contract NAS3-6013 under the technical management of Mr. Henry B. Tryon and consultation with Mr. Harold E. Rohlik, NASA Lewis Research Center, Cleveland, Ohio. It describes the design and mechanical testing of the turbine research package in accordance with Article I, Section B of the contract.

TABLE OF CONTENTS

LIST OF FIGURES

LIST OF FIGURES

LIST OF FIGURES

LIST OF TABLES

I. SUMMARY

The turbine research package is a test rig intended to provide cold-flow aerodynamic performance data for the Brayton-cycle alternator drive turbine. This turbine is a two-stage, axial-flow unit designed to provide a high efficiency potential.

The turbine research package was designed to provide a convenient mechanical configuration for aerodynamic testing. This unit has been constructed and tested mechanically to twenty percent over its design speed. It has demonstrated satisfactory mechanical characteristics and completed the required acceptance test. The National Aeronautics and Space Administration will conduct aerodynamic testing at the Lewis Research Center. The turbine research package was delivered to NASA on January 26, 1966.

II. INTRODUCTION

NASA is conducting an evaluation program of candidate Brayton-cycle turbomachinery configurations. As a part of this program, Pratt & Whitney Aircraft is to design, fabricate, and deliver a turboalternator incorporating a two-stage, axial-flow turbine and a 15 KVA, 4-pole inductor alternator supported on gas bearings. The turbine for the turboalternator is designed to provide high efficiency and reliability potential. The specific turbine design conditions for the turboalternator are as follows.

Working fluid	Argon	Total pressure ratio	1.26
Flow rate (lb/sec)	0.611	Operating life (hours)	10,000
Inlet total temperature (°R)	1685	Rotational speed (rpm)	12,000
Inlet total pressure (psia)	8.45	Maximum speed (rpm)	14,400

The rotational speed was selected to provide 400-cycle-per-second, three-phase, alternating current electric power using a four-pole alternator.

A turbine research package incorporating oil lubricated, rolling contact bearings is also provided to permit evaluation of the aerodynamic performance of the turbine using low-temperature gas.

Since the turbine research package is a cold-flow rig, its operating conditions differ from those of the actual turbine so that an accurate aerodynamic simulation is achieved. The design conditions for the turbine research package are:

Working fluid	Argon	Total pressure ratio	1.26
Flow rate (lb/sec)	1.10	Rotational speed (rpm)	6680
Inlet total temperature (°R)	520	Maximum speed (rpm)	8020
Inlet total pressure (psia)	8.45		

The turbine research package is actually able to operate with inlet temperatures up to 710°R, inlet pressures up to 23 psia, and rotational speeds up to 9350 rpm. The complete turbine research package is shown in Figures 1 and 2.

The discussion that follows begins with a description of the turboalternator turbine design because of the dependence of the turbine research package design on the turboalternator turbine design. This is followed by a description of the turbine research package and then by a presentation and discussion of the results of the mechanical acceptance test.

III. TURBINE AERODYNAMIC DESIGN

The turbine blading for the Brayton-cycle turboalternator was selected with the objective of producing high efficiency and high reliability. Since the speed and temperature in the turboalternator are relatively low, the mechanical design of the turbine can incorporate large design margins to provide high reliability potential. A high velocity ratio * turbine was selected to provide high efficiency potential. Rather than using a large-diameter, single-stage turbine with short blades, a two-stage turbine was chosen to maintain a reasonable blade height to reduce tip clearance and end losses. The effort to maintain reasonable blade heights coupled with low gas flow in the Brayton cycle led to a low axial velocity-to-wheel speed ratio. This design results in a turbine with high reaction which is consistent with the high velocity ratio selected.

The thermodynamic design parameters of the turbine are presented in Table I. The predicted efficiencies are based on conservative loss

TABLE I

Brayton Cycle Turboalternator
Turbine Thermodynamic Design

	First Stage	Second Stage	Over-All
Work, Btu/lb	7.52	7.52	15.04
Rotational speed, rpm	12,000	12,000	12,000
Pressure ratio across turbine			
Total to total	1.1144	1.1190	1.2469
Total to static			1.2542
Pressure ratio, flange to flange			
Total to total			1.2495
Total to static			1.2540
Mean velocity ratio (actual)	0.726	0.724	0.725
Axial gas velocity-to-mean-blade velocity	0.334	0.3375	
Stage exit axial mach number	0.0809	0.0833	
Total to total efficiency	0.8473	0.8472	0.8501
Total to static efficiency	0.8050	0.8026	0.8254
Exit swirl angle (mean), degrees	-4.61	-4.56	
Hub-to-tip ratio	0.746	0.730	
Blade root static pressure ratio	1.0363	1.0356	
Flange to flange, total to total efficiency			0.8428
Flange to flange, total to static efficiency			0.8264

*Velocity ratio, ν, is defined as the ratio of mean wheel linear speed, U, to the square root of twice the actual turbine work. Hence, $\nu = U/\sqrt{2\Delta h}$. For multistage turbines, the over-all velocity ratio is defined as ${}^{o}\nu = \sqrt{\Sigma U^2 / 2\Delta h_o}$ where Δh_o is the actual over-all turbine work.

coefficients which were adjusted by a 1/5 power law to account for the effect of low Reynolds numbers. (The Reynolds numbers for both the nozzles and blades based on the axial projection of the chord are a little over 13,000.) Gas leakage over the blade tips is estimated to be approximately 4 percent of the primary flow.

The thermodynamic conditions and gas angles relative to the plane of rotation entering and leaving each airfoil row at root, mean, and tip locations are presented in Table 2. This table lists conditions, averaged circumferentially, immediately upstream and forward of the leading edge or immediately downstream of the trailing edge of the blades and vanes. The fluid conditions in Table 2 represent the main stream, except for the conditions under "Leaving Turbine." At this position, complete mixing of the leakage with the main stream flow is assumed. Nomenclature for the gas triangles is shown in Figure 3. The selected gas triangles employ free vortex flow patterns. There is a small amount of swirl left in the gas at the exit of the turbine in the direction of rotation. This condition was selected to provide balance between the reaction at the blade roots and nozzle tips and to provide high efficiency potential.

The airfoil geometries are presented in Figures 4 through 7. The airfoil contours were selected to provide conservative distributions within the passages. These distributions are shown in Figures 8 through 13 for the vanes and Figures 14 through 17 for the blades. High convergence and low diffusion rates are characteristic of the airfoil designs. At the blade tip sections, the wide spacing between airfoils prevented the application of two-dimensional channel analysis to determine the velocity distribution.

A summary of the airfoil dimensions and stresses in the turbine of the turboalternator is presented in Table 3. The first-stage vane operates at an average metal temperature of 1685°F, and the second-stage vane operates at an average metal temperature of 1624°R. As shown in Table 3, the bending stresses are very low. With the use of AMS 5382 material for the vanes, a very large design margin is provided. At 1660°R, the yield strength for this material is 35,000 psi, and the 1 percent creep strength for 10,000 hours is 28,500 psi. The maximum bending stress to which the vanes will be subjected is only 153 psi.

Blade stresses are also shown in Table 3 for conditions in the turboalternator. The primary stresses are due to centrifugal pull, with the gas bending stresses being almost insignificant. Centrifugal bending stresses are induced, however, because it was not possible to stack the centers of gravity of all sections on a radial line and still obtain the required blade shape. These stresses are shown in Figures 19 and

TABLE 2

Turboalternator Turbine Gas Triangles

Radial Station		First Stage Root	First Stage Mean	First Stage Tip	Second Stage Root	Second Stage Mean	Second Stage Tip
Entering Vane							
Total temperature	°R	1685	1685	1685	1624.48	1624.48	1624.48
Total pressure	psfa	1217	1217	1217	1092.11	1092.11	1092.11
Static temperature	°R	1681.2	1681.3	1681.3	1620.9	1620.9	1620.9
Static pressure	psfa	1210.2	1210.3	1210.3	1086.1	1086.1	1086.1
Axial velocity - C_x	ft/sec	149.3	149.3	149.3	148.4	148.4	148.4
Absolute swirl velocity - C_{uo}	ft/sec	-36.9	-31.7	-27.7	-14.0	-11.9	-10.4
Gas inlet angle - α_o	degrees	103.9	102.0	100.5	95.38	94.61	93.97
Leaving Vane							
Static temperature	°R	1636.8	1648.5	1656.2	1575.2	1587.9	1596.0
Static pressure	psfa	1125.9	1146.1	1159.4	1005.3	1025.7	1038.8
Axial velocity - C_x	ft/sec	151.5	151.5	151.5	153.2	153.2	153.2
Absolute swirl velocity - C_{u1}	ft/sec	526.2	451.7	395.7	532.4	451.8	392.3
Gas exit angle - α_1	degrees	16.07	18.54	20.96	16.05	18.73	21.33
Reynolds number			1.359×10^4			1.378×10^4	
Flow area	ft^2		0.0717			0.0767	
Entering Blade							
Relative total temperature	°R	1643.5	1652.05	1661.94	1582.45	1591.53	1602.15
Relative total pressure	psfa	1137.35	1153.2	1169.53	1016.89	1031.54	1048.83
Static temperature	°R	1636.64	1648.76	1656.57	1574.91	1588.17	1596.45
Static pressure	psfa	1125.52	1146.47	1160.11	1004.82	1026.1	1039.52
Axial velocity - C_x	ft/sec		143.04			144.41	
Relative swirl velocity - W_{u2}	ft/sec	149.29	7.98	-113.88	161.53	9.02	-121.04
Wheel speed - U_2	ft/sec	380.55	445.06	509.57	375.0	444.07	513.13
Gas inlet angle - β_2	degrees	43.78	86.82	128.51	41.81	86.44	129.95
Leaving Blade							
Static temperature	°R	1618.47	1618.48	1618.48	1558.01	1558.02	1558.02
Static pressure	psfa	1086.12	1086.13	1086.14	970.31	970.32	970.33
Axial velocity - C_x	ft/sec	148.21	148.21	148.21	149.81	149.81	149.81
Relative swirl velocity - W_{u3}	ft/sec	365.95	432.57	498.66	360.25	431.6	502.34
Wheel speed - U_3	ft/sec	380.55	445.06	509.57	375.0	444.07	513.13
Gas exit angle - β_3	degrees	22.05	18.92	16.56	22.59	19.14	16.61
Reynolds number			1.300×10^4			1.343×10^4	
Actual flow area	ft^2		0.0743			0.0800	
Leaving Turbine							
Total temperature	°R				1563.97	1563.97	1563.97
Static temperature	°R				1560.32	1560.33	1560.34
Total pressure	psfa				975.99	975.99	975.99
Axial velocity - C_x	ft/sec				150.04	150.04	150.04
Absolute swirl velocity - C_{u3}	ft/sec				-14.21	-12.00	-10.38
Absolute gas exit angle	degrees				95.42	94.58	93.96

TABLE 3

Turboalternator Turbine Airfoil Dimensions and Stresses

Radial Station		First Stage Root	First Stage Mean	First Stage Tip	Second Stage Root	Second Stage Mean	Second Stage Tip
Vanes							
Number of Vanes			44			40	
Material			AMS 5382			AMS 5382	
Diameter	in	7.318	8.525	9.732	7.218	8.5045	9.791
Average radial height	in		1.207			1.2865	
Pitch	in	0.5225	0.6087	0.6947	0.553	0.651	0.750
Axial width	in	0.518	0.6035	0.689	0.5546	0.6528	0.7511
Vane chord	in	0.860	0.958	1.064	0.874	1.015	1.158
Solidity		1.647	1.575	1.533	1.58	1.559	1.542
Gas bending stress	psi	0	117.7	0	0	41.1	152.7
Airfoil metal temperature	°R	1684.5	1684.6	1684.6	1624.1	1624.1	1624.1
Total axial thrust on	lb		14.1			11.91	
airfoils			9.65			8.33	
Total tangential load	lb						
Blades							
Number of blades			36			36	
Material			PWA-1010			PWA-1010	
Diameter	in	7.268	8.500	9.732	7.162	8.481	9.800
Average radial height	in		1.232			1.319	
Pitch	in	0.635	0.7404	0.846	0.6245	0.7401	0.8552
Axial width	in	0.825	0.616	0.407	0.899	0.6595	0.420
Blade chord	in	0.953	0.975	0.984	1.005	1.019	1.011
Solidity		1.5	1.318	1.162	1.61	1.377	1.182
Centrifugal stress	psi	3793	2536	0	3715	2620	0
Gas bending stress	psi	71.0	64.0	0	56	88	0
Resultant bending stress (Gas and misalignment bending)	psi	777	317.7	0	1630	1643	0
Airfoil metal temperature	°R	1642.7	1651.7	1661.3	1581.5	1591.1	1601.5
Total axial thrust	lb		13.7			13.5	
Total tangential load	lb		8.35			8.36	

20. The material selected for the turboalternator turbine blades is PWA-1010, which is a nickel alloy equivalent to Inconel 718. With the use of this material, a very large design margin is provided. The 0.1 percent creep strength in 10,000 hours for the material is about 35,000 psi, and the maximum stress in the turbine blades is only 5,400 psi.

The predicted over-all performance of the turbine at a variety of velocity ratios is presented in Figure 21, and the flow parameter is presented in Figure 22 as a function of pressure ratio. These data are based on operation with design turbine inlet temperature and pressure. At significantly lower pressure, Reynolds number effects would be expected to change the predicted values.

IV. DESCRIPTION OF TURBINE RESEARCH PACKAGE

The turbine research package is designed to provide a convenient means of evaluating the aerodynamic performance of the turboalternator turbine using low-temperature gas. A cross-sectional drawing of the turbine research package is presented in Figure 23. The argon enters the inlet case (shown in Figure 24) and passes through pre-rotation vanes (Figure 25) which add swirl to the inlet gas to simulate the turbine-compressor exhaust. Flow continues through the two turbine stages (Figures 26 through 29) and exhausts through the exit diffuser and scroll (Figure 30). The turbine blades are integrally machined on each disk for each stage, and the two disks are bolted to the main disk shown in Figure 31. The main disk, in turn, is bolted to the shaft assembly (see Figure 32.). An interstage labyrinth seal (Figure 33) is located between the two disks. The shaft is supported by a roller bearing and a ball bearing which are jet-oil lubricated. The bearing compartment is sealed by a carbon face seal on the turbine end and a labyrinth seal on the drive end (see Figure 34). The main bearing housing is shown in Figures 35 and 36 and includes a breather fitting as well as oil inlet and scavenge ports.

The turbine research package can be assembled in two alternate configurations. The first stage can be assembled without the second-stage nozzle vane and rotor for detailed aerodynamic performance testing of the first stage. Extra duct assemblies are provided to form smooth gas-path walls with this configuration. As a second alternative, dummy wheels can be installed in place of both bladed disks for friction power calibration tests. These wheels have the same weight as the bladed disks. The second-stage dummy wheel is shown in Figure 37.

The aerodynamic instrumentation provided is shown in Table 4.

Both the roller bearing and the ball bearing (see Figures 38 and 39) have an inner diameter of 20 millimeters and an outer diameter of 42 millimeters. The bearings are made of AMS 6444 steel and have silver-plated steel cages. Each bearing is cooled and lubricated by MIL-L-7808 lubricant or by an appropriate oil with similar characteristics at the operating conditions. A thermal map is presented in Figure 40 showing the predicted operating temperatures in the bearing area with an argon inlet temperature of 250°F and an oil inlet temperature of 80°F. Three iron-constantan thermocouples are located in the housing of each bearing to monitor bearing outer-race temperatures. Oil is metered to the bearings through 0.039-inch diameter orifices which results in an oil flow rate of 1.0 lb/min for each bearing.

TABLE 4

Aerodynamic Instrumentation Provisions

Location	Static Pressure Taps	Other Provisions
Plane of three inlet struts	Four in the inner wall and four in the outer wall	One radial traverse boss. Six 1/4-in. dia. holes for fixed probes
Interstage	Four in the outer wall of each of the locations downstream of the first-stage nozzle, the first-stage rotor, and the second-stage nozzle. Four in the cavity upstream of the first-stage disk	One radial traverse boss in leading edge plane of second nozzle for use with second stage removed
Exit plane (downstream of second-stage rotor)	Four in the inner wall and four in the outer wall	One radial traverse boss
Scroll radial section	Fourteen taps spaced at one-inch intervals in two rows approximately 180° apart	
Scroll exit	Four	Four 1/4-in. dia. holes for fixed probes

Bearing oil compartment design parameters are presented below:

Oil supply pressure (psia)	35
Bearing compartment pressure (psia)	6.0
Rear labyrinth seal	
Radial clearance (inch)	0.010
Leakage flow (lb/sec of air)	0.006

The bearings used in the turbine research package are identical to those used in the turbine-compressor turbine research package which is designed to operate at 26,000 rpm. The DN factor for the bearings (bearing inner diameter times design speed) in the turbine research package is 135,000 mm rpm, which represents a conservative application for these bearings. With mechanical unbalance of 0.1 oz. in. and with an aerodynamic thrust of 60 pounds on the ball bearing, the predicted B-10 fatigue life* of the bearings is 24,000 hours, but this value has little meaning except that a bearing fatigue failure is highly unlikely.

The interface between the argon and the bearing compartment is sealed by a carbon face seal which is held in contact with a rotating seal plate by a spring. An O-ring serves as the static secondary seal. The bearing compartment pressure should not be set below 2 psia to avoid oil foaming. Whenever practical, the bearing compartment pressure should be approximately equal to the turbine discharge pressure to

*The B-10 life is the time required to fail 10 percent of the bearings of a given type in a given application.

reduce the pressure drop across the carbon face seal. The bearing compartment breather pipe can be connected to the turbine exhaust piping in order to provide the recommended bearing compartment pressure. The oil should be supplied at a pressure between 29 and 35 psi above the bearing compartment pressure. The other end of the shaft is sealed with a five-lip staggered labyrinth seal. The labyrinth seal was selected for use at this location to reduce the parasitic power consumption.

The heat loss rates from the gas path during operation without rig insulation were determined for an inlet temperature of 250°F and an inlet pressure of 8.45 psia. These values are presented below:

	Heat Loss Rate (Btu/hr)
Inlet annulus	190
Turbine case	159
Exhaust annulus	203
Exhaust scroll	418
Oil	36
Total heat loss rate	1006

These values do not include the heat generated in the bearings and seals which is carried away by the oil. The "oil" entry indicates that 36 Btu/hr is transferred from the gas path to the oil during operation. The total heat loss during operation without insulation represents about 2.8 percent of the turbine output power, and, therefore, will significantly affect the measured turbine efficiency. Consequently, operation with rig insulation is recommended.

The static structure and rotating parts are conservatively designed and have ample design margins. Rotor critical speeds for two rotor configurations were determined and are presented in Figure 41. The increase in critical speed with rotor speed is a result of gyroscopic stiffening. As shown, all critical speeds are well above the maximum design speed of 8020 rpm. If the turbine research package is operated at 9350 rpm, which corresponds to 20 percent overspeed with an inlet temperature of 710°R, ample critical speed margin is provided. The first critical speed is reached with a rotor speed of 17,800 rpm for the two-stage rotor and 19,500 rpm for the single-stage rotor. The second critical speed is encountered at 22,680 rpm for the two-stage rotor and 24,000 rpm for the single-stage rotor. All of these critical speeds are bent-shaft modes.

The turbine research package employs the same airfoil and wall contours as are provided in the turboalternator package. Since the turbine research package operates with relatively low gas temperature at low speed, smaller clearances can be employed than are possible in the hot turboalternator. In order to permit simple modifications in the turbine research package to evaluate blade tip clearance effects, the turbine research package was designed with smaller clearances than the turboalternator. Although the turboalternator operating clearance is conservatively set at 0.030 to 0.032 inch to allow for various thermal conditions, the turbine research package is constructed with a blade tip clearance of approximately 0.010 inch. Research package clearances can be subsequently increased by machining the blade tips. The position of the rotor at various operating speeds was analyzed to ensure that adequate local clearances existed. This analysis included the effects of centrifugal growth of the rotor, bearing radial clearance, rotor mechanical unbalance, and shaft deflection. The results of the analysis are presented in Figure 42. At design speed with the maximum allowable mechanical unbalance of 0.1 ounce-inch, the rotor excursion will result in a local clearance reduction of less than 0.0035 inch. The minimum radial blade tip clearance based on tolerances and with a 520°R inlet total temperature is 0.008 inch. With a 710°R inlet temperature, the minimum clearance is slightly larger. Therefore, ample clearance margin is provided. Measurements of the actual clearances in the turbine research package are included in the Appendix.

The turbine research package operates with cool gas and at speeds lower than the turboalternator design conditions; therefore, the stress in the blades and vanes are significantly lower than in the turboalternator. Since there is ample margin in the turboalternator design as discussed in Section III above, there is greater margin in the turbine research package. The vanes in the turbine research package are constructed of the same material as in the turboalternator. The disk and integrally machined blades are constructed of AMS 5660 which has a yield strength of 76,000 psi. The average tangential stress of the disk is 8650 psi at 9350 rpm. The maximum stresses in the disk and at the attachment between the shaft and the disk are well below the material yield stress at the maximum anticipated speed.

V. TEST PROGRAM

A. INTRODUCTION

The aerodynamic testing of the Brayton-cycle turboalternator turbine will be conducted at the Lewis Research Center. No aerodynamic tests were conducted at Pratt & Whitney Aircraft. A test program was conducted to verify satisfactory mechanical operation of the turbine research package. These tests were conducted in two phases: First, the rotor dynamic performance was evaluated to ensure proper rotor behavior. Then the research package was subjected to an acceptance test to demonstrate satisfactory mechanical characteristics. The acceptance test consisted of running the turbine at the design speed (6680 rpm) for thirty minutes and at 120 percent of design speed for ten minutes.

B. TEST FACILITY

The test stand used for testing the turbine research package is shown in Figures 43 and 44. The test was controlled remotely from the control room shown in Figure 45. Air was supplied to the turbine inlet through pressure reduction and control valves. Drive air from the turbine was exhausted directly to the ambient environment. The oil lubrication system consisted of motor-driven supply and scavenge pumps, a reservoir, strainer and filter, and a control valve. The bearing compartment was vented to the ambient environment.

Vibration pickups (Consolidated Electrodynamics Corporation Type 4-H8-0001) were used to measure the vibration of the static cases at the drive end of the main bearing housing and at the inlet flange of the turbine exhaust case. Measurements were made for vibration in both the horizontal and vertical directions. Signals from the pickups were read on meters designed by Pratt & Whitney Aircraft and capable of measuring vibrations with amplitudes up to 0.0025 inch.

Rotor speed was sensed by five Electro-Products Laboratories Model 3016 magnetic speed pickups. The outputs of the pickups were read on a Hewlett-Packard counter and a General Radio counter used in conjunction with a selector switch.

Temperatures of the bearings and the lubricating oil at the inlet and outlet were sensed by thermocouples, with the thermocouple output being read on Brown potentiometers.

C. ROTOR DYNAMIC TEST

The dynamic operating characteristics of the rotor were measured to ensure proper mechanical operation of the turbine research package. The radial motion of the first-stage disk was sensed by eddy-current-type proximity probes (Bentley Model H-3-021-4). The probes were positioned 90 degrees apart (as shown in Figure 46) and were connected to the x and y axes of an oscilloscope to display the shaft orbit. Another proximity probe was used to measure the radial motion of the six-tooth speed pick-up gear at the other end of the shaft.

Testing was conducted at 1500, 7200, and 8600 rpm. The test results obtained at 1500 rpm are shown in Figure 47. At this speed, the orbit and radial motion are the result of the radial clearance in the roller bearing increased proportionately by the axial distance between the probe and the bearing. As shown, the orbit radius is about 0.001 inch and the radial motion of the six-tooth gear is about 0.0002 inch. The results obtained at 7200 and 8600 rpm are shown in Figures 48 and 49, respectively. The orbit radius is about 0.0015 inch at 7200 rpm and 0.002 inch at 8600 rpm, which are less than the predicted motion shown in Figure 42. The radial motion of the six-tooth gear increased by 0.0003 inch to a total of 0.0005 inch.

The results of these tests indicate that the rotor dynamic behavior is satisfactory.

D. ACCEPTANCE TEST

An acceptance test of the turbine research package to demonstrate the mechanical integrity of the unit was required. The specified acceptance test consisted of acceleration to design speed (6680 rpm) and operation at this speed for 30 minutes, acceleration to 120 percent of design speed (8020 rpm) and operation at this speed for 10 minutes, and deceleration. The test was specified as a free spin-up, and, therefore, no load was applied to the shaft.

The acceptance test was successfully completed on January 20, 1966. The vibration pickups indicated a maximum motion of 0.00005 inch amplitude. This value was measured in the vertical plane at the drive end of the bearing housing. Maximum ball and roller temperatures were 164°F and 149°F, respectively. Bearing temperatures were consistently lower than the inlet oil temperature, which indicates that heat is lost from the housing to the test cell and to the drive air. These measurements were substantially in agreement with the data recorded during the rotor dynamic test.

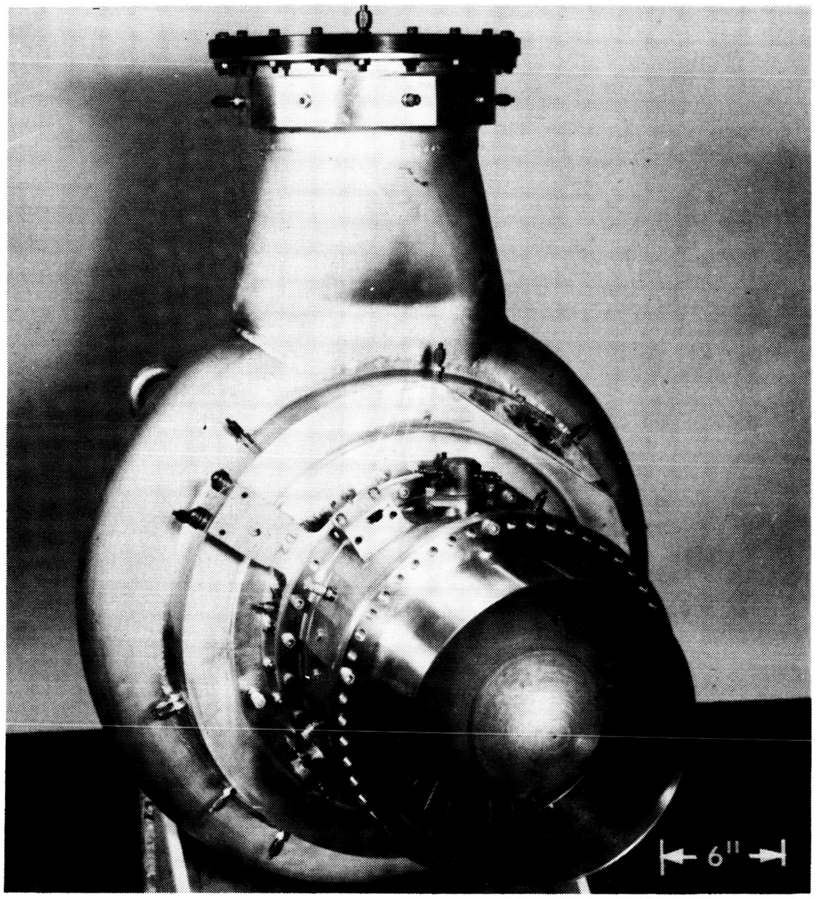

M-36640

Figure 1 Gas Inlet End of Turbine Research Package

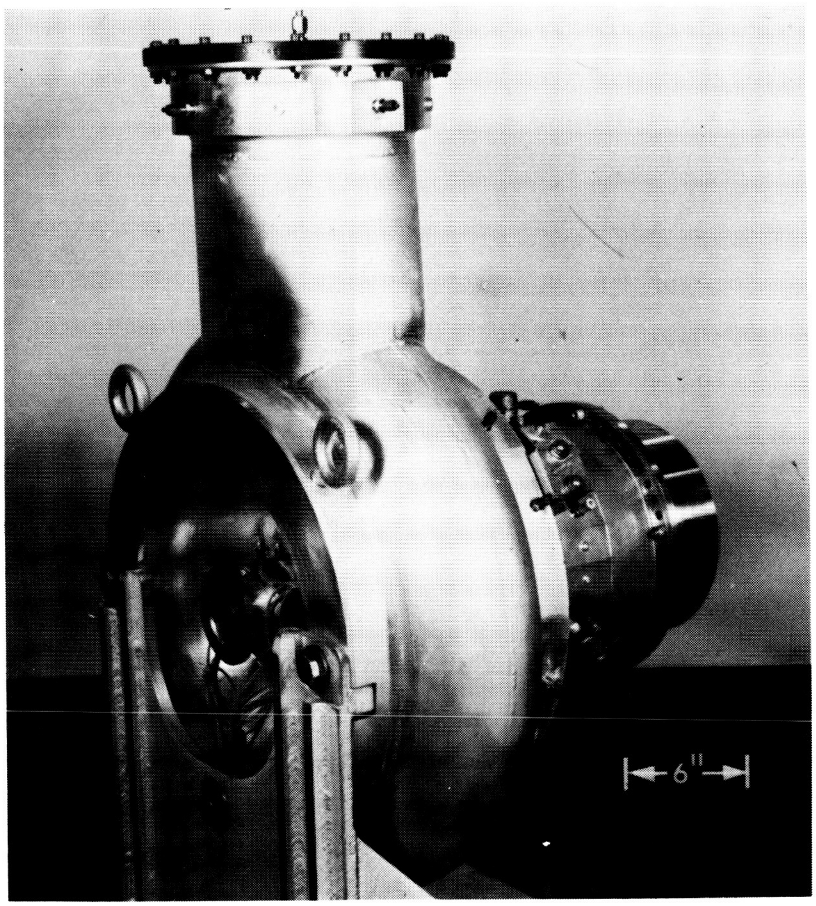

M-36640

Figure 2 Drive End of Turbine Research Package

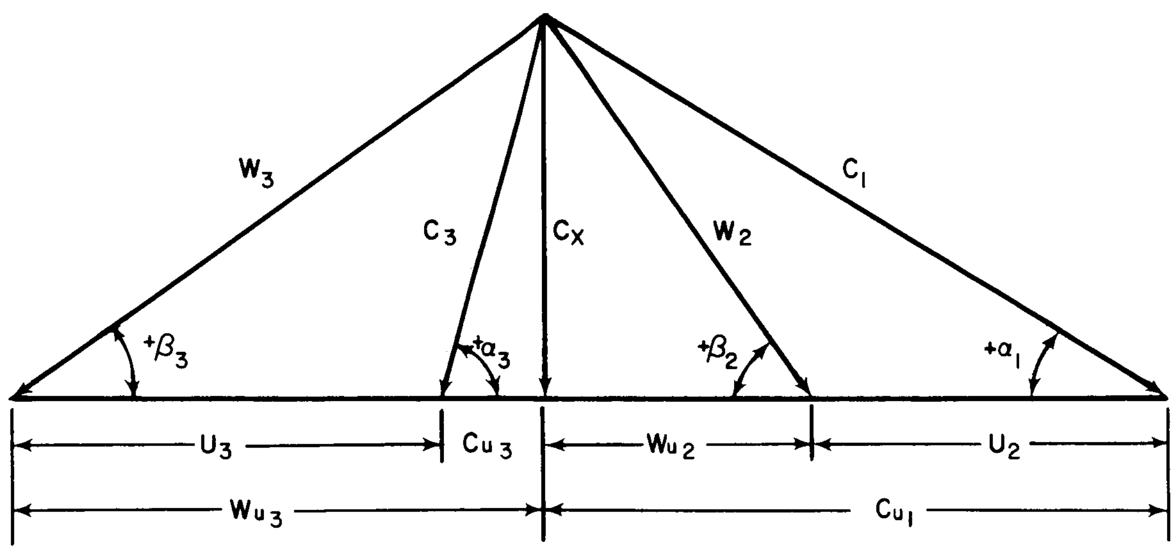

C - ABSOLUTE GAS VELOCITY, FT/SEC
U - BLADE VELOCITY, FT/SEC
W - RELATIVE GAS VELOCITY, FT/SEC
α - ABSOLUTE GAS ANGLE MEASURED FROM PLANE OF ROTATION
β - RELATIVE GAS ANGLE MEASURED FROM PLANE OF ROTATION

SUBSCRIPTS

1 - STATION AT NOZZLE TRAILING EDGE
2 - STATION AT ROTOR LEADING EDGE
3 - STATION AT ROTOR TRAILING EDGE
X - AXIAL

Figure 3 Turbine Velocity Triangle Nomenclature

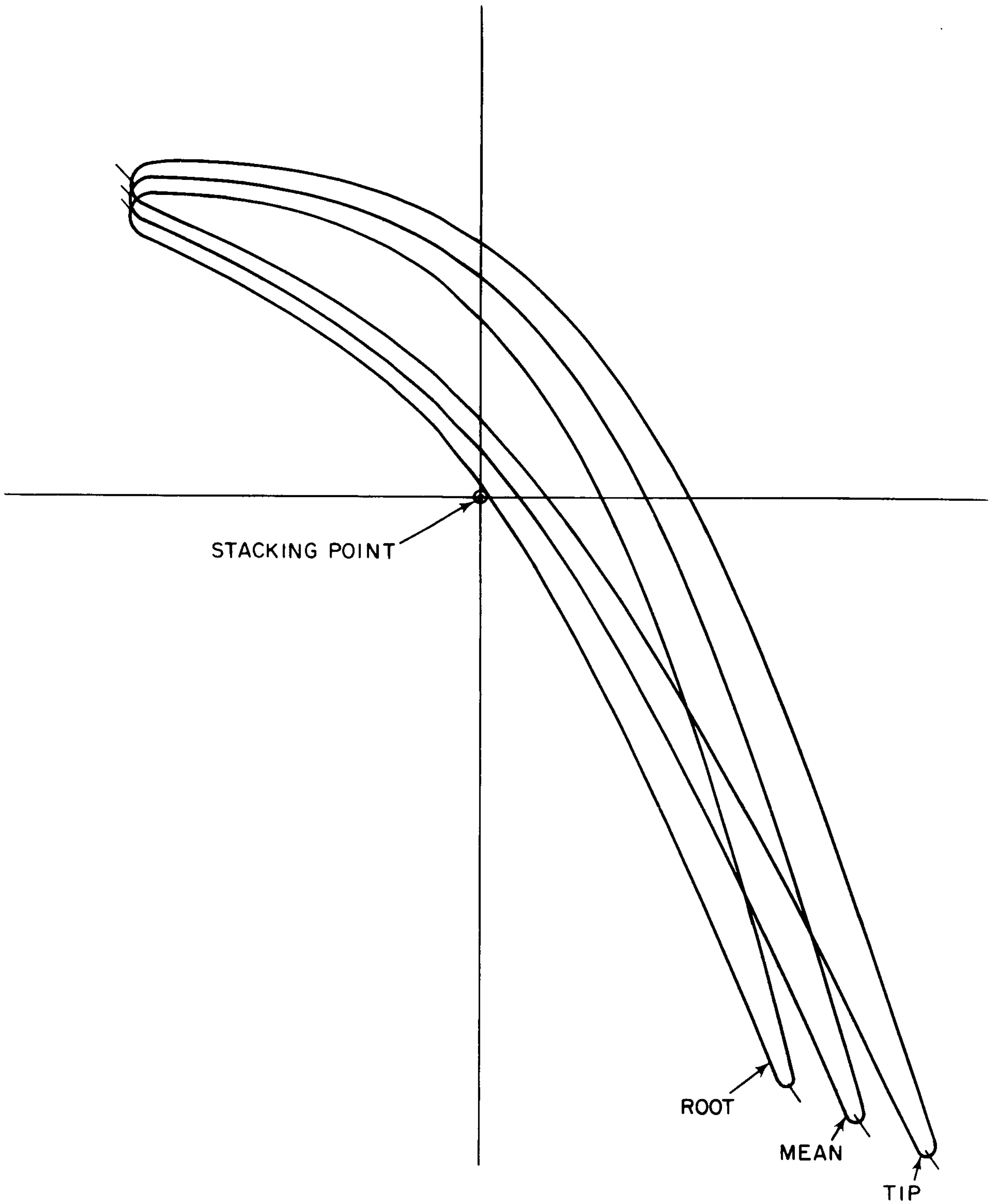

Figure 4 First-Stage Turbine Vane Airfoil Geometry

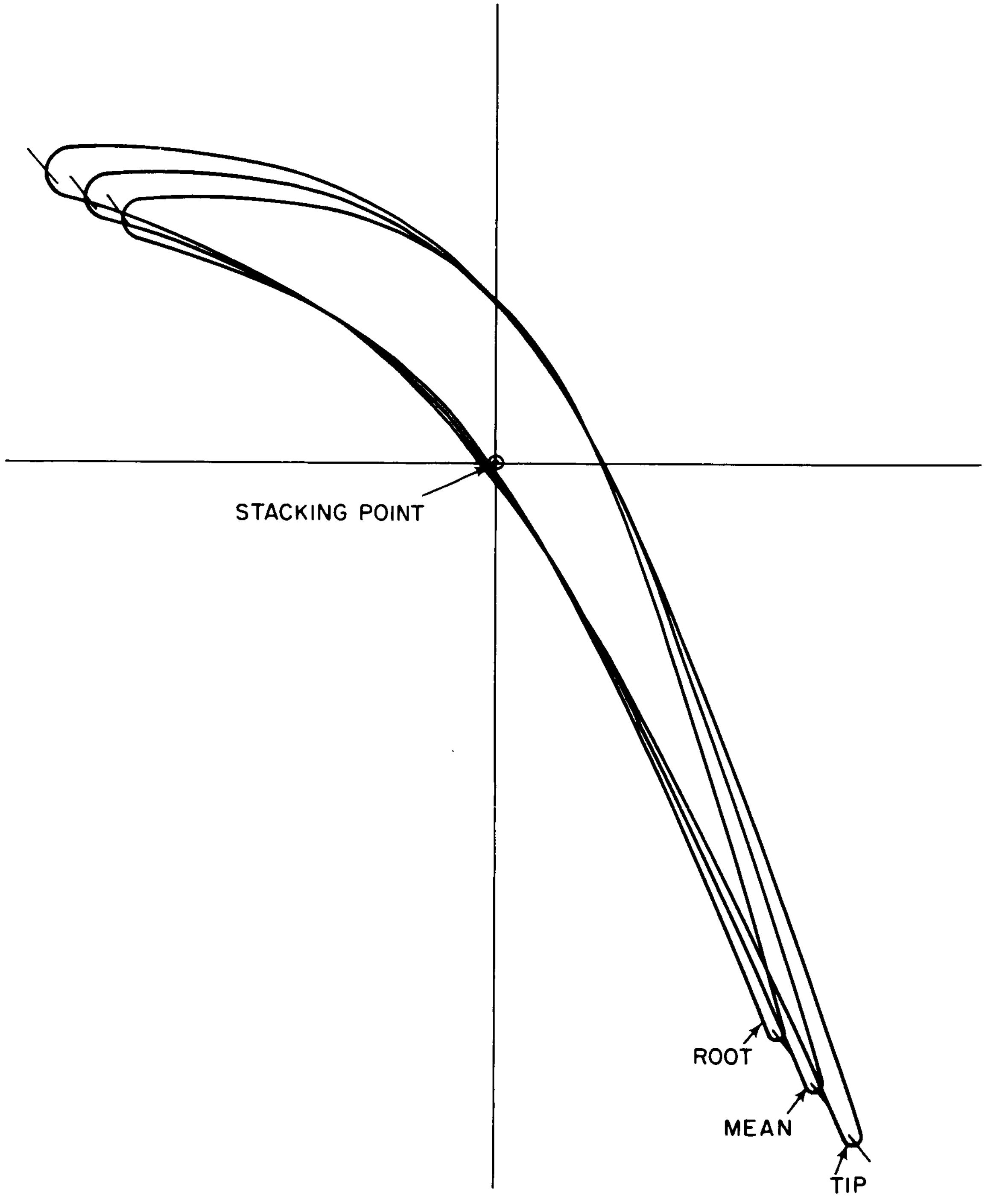

Figure 5 Second-Stage Turbine Vane Airfoil Geometry

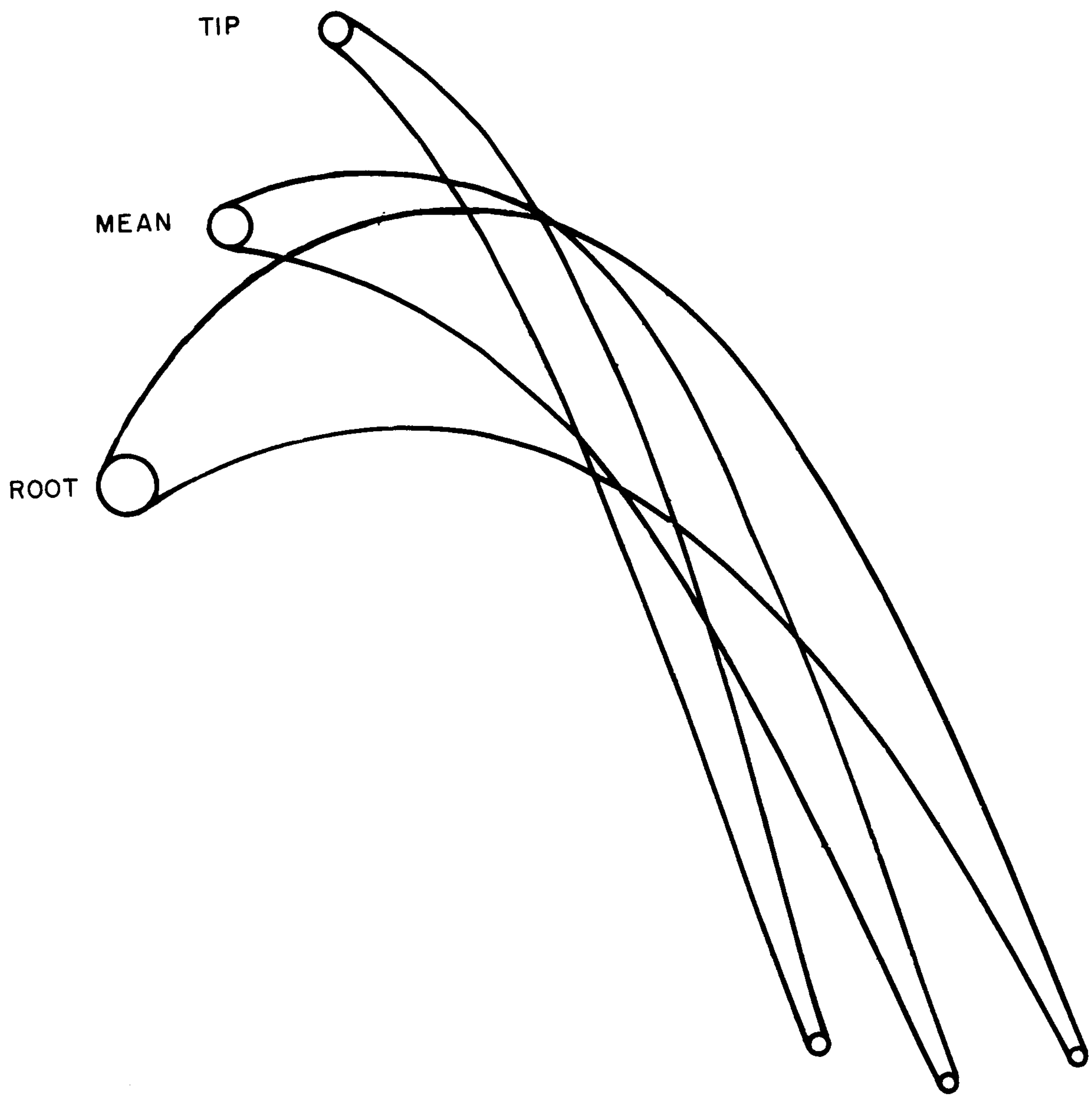

Figure 6 First-Stage Turbine Blade Airfoil Geometry

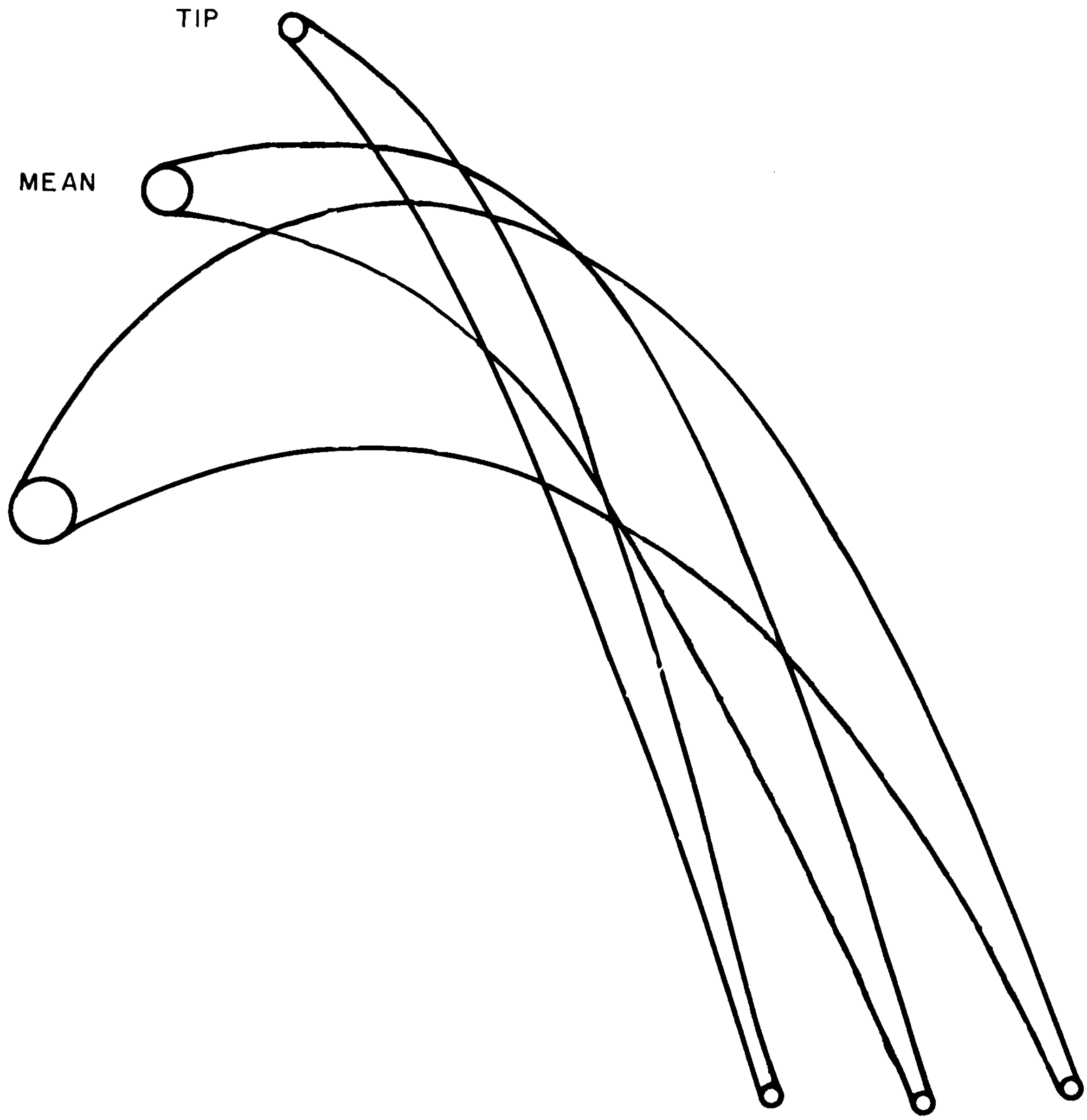

Figure 7 Second-Stage Turbine Blade Airfoil Geometry

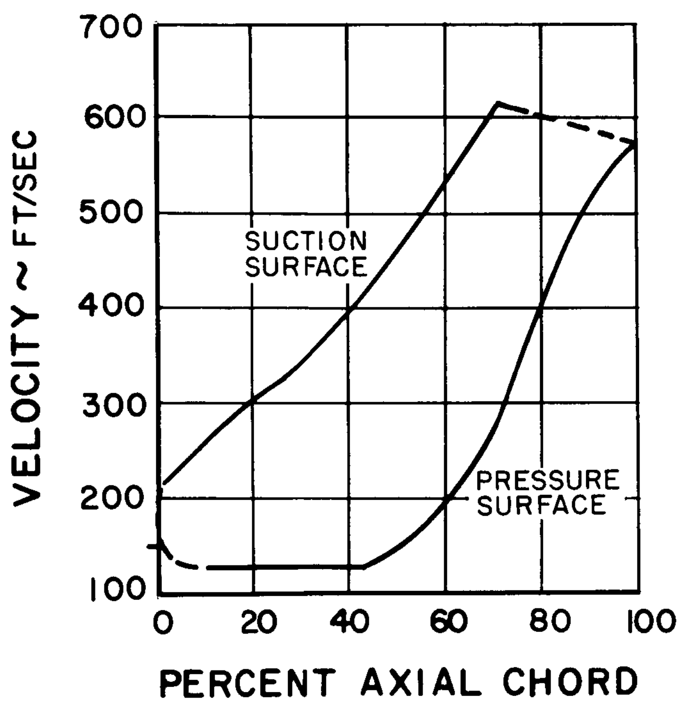

Figure 8 Velocity Distribution at Root Section of Turboalternator First-Stage Vane

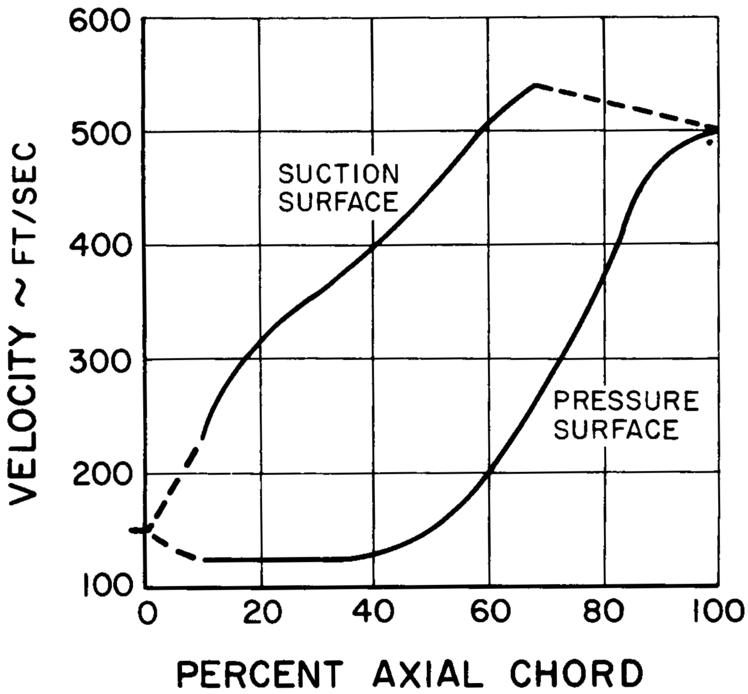

Figure 9 Velocity Distribution at Mean Section of Turboalternator First-Stage Vane

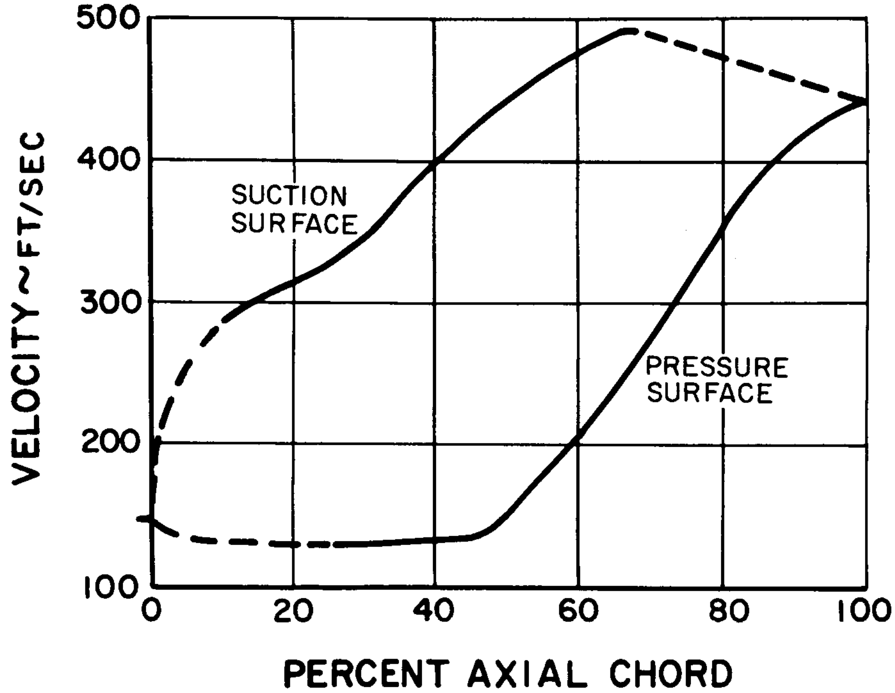

Figure 10 Velocity Distribution at Tip Section of Turboalternator First-Stage Vane

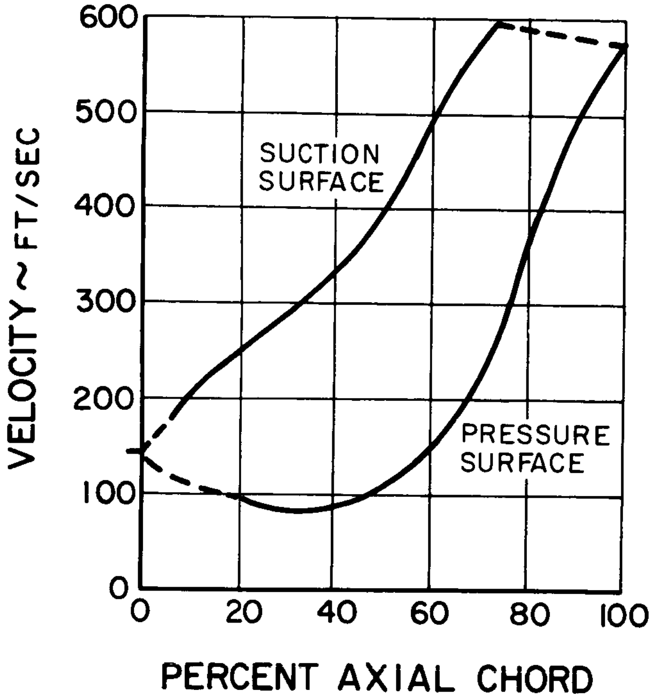

Figure 11 Velocity Distribution at Root Section of Turboalternator Second-Stage Vane

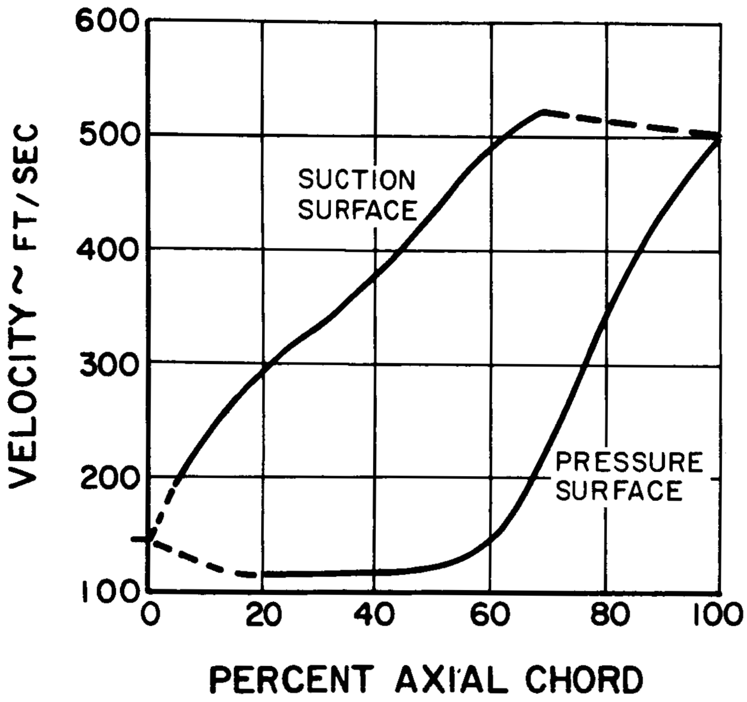

Figure 12 Velocity Distribution at Mean Section of Turboalternator Second-Stage Vane

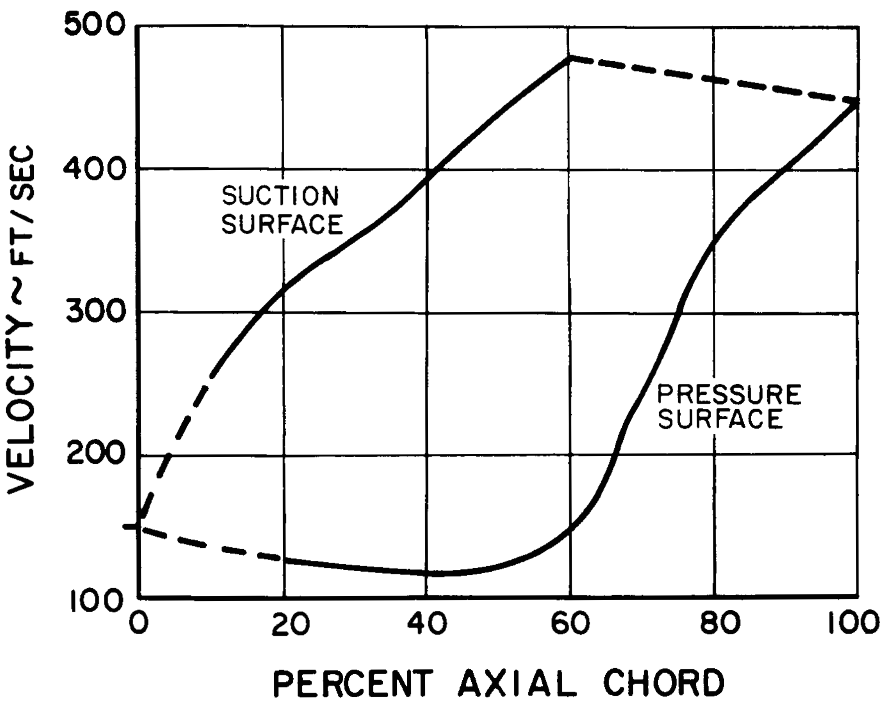

Figure 13 Velocity Distribution at Tip Section of Turboalternator Second-Stage Vane

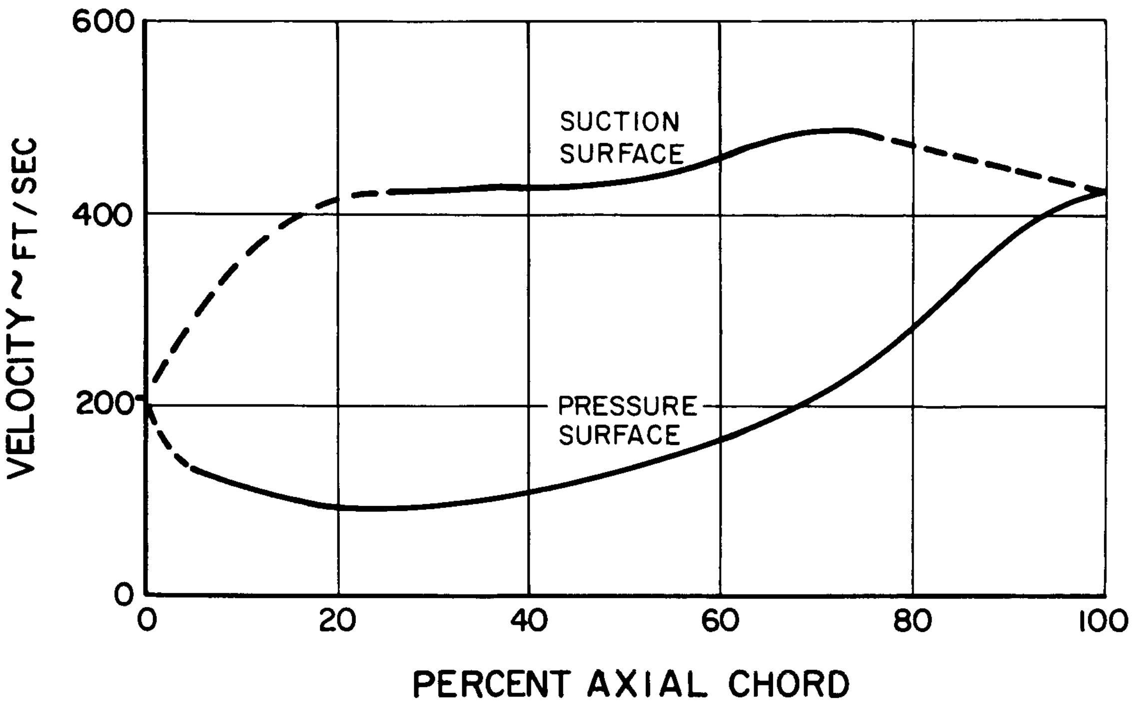

Figure 14 Velocity Distribution at Root Section of Turboalternator First-Stage Blade

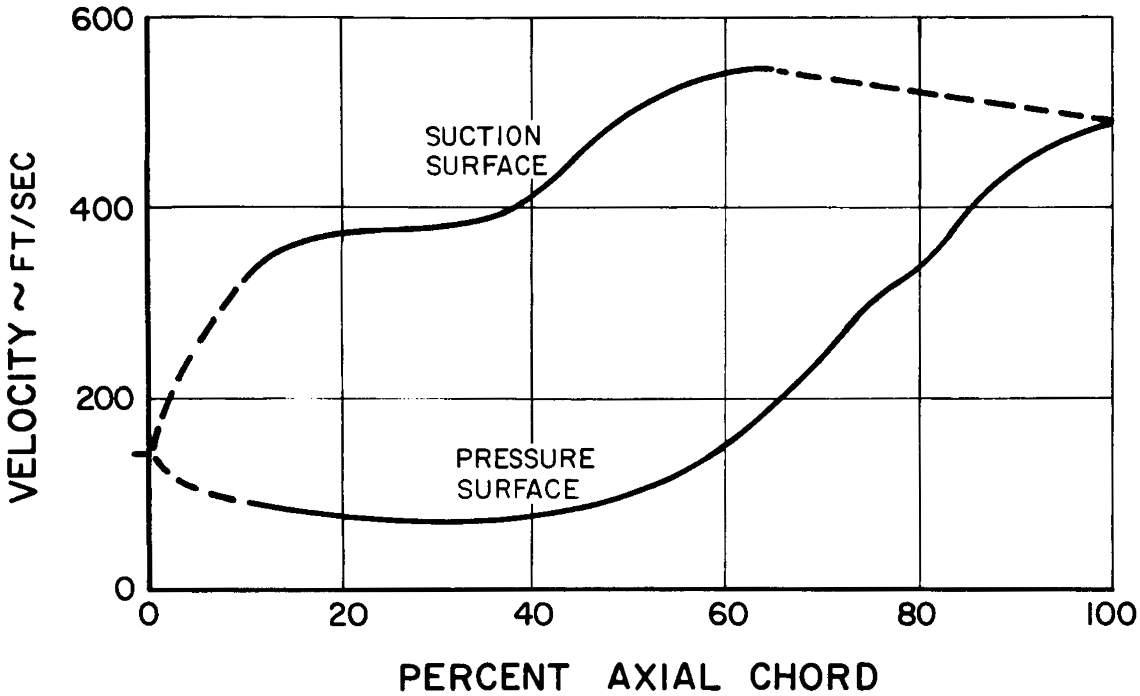

Figure 15 Velocity Distribution at Mean Section of Turboalternator First-Stage Blade

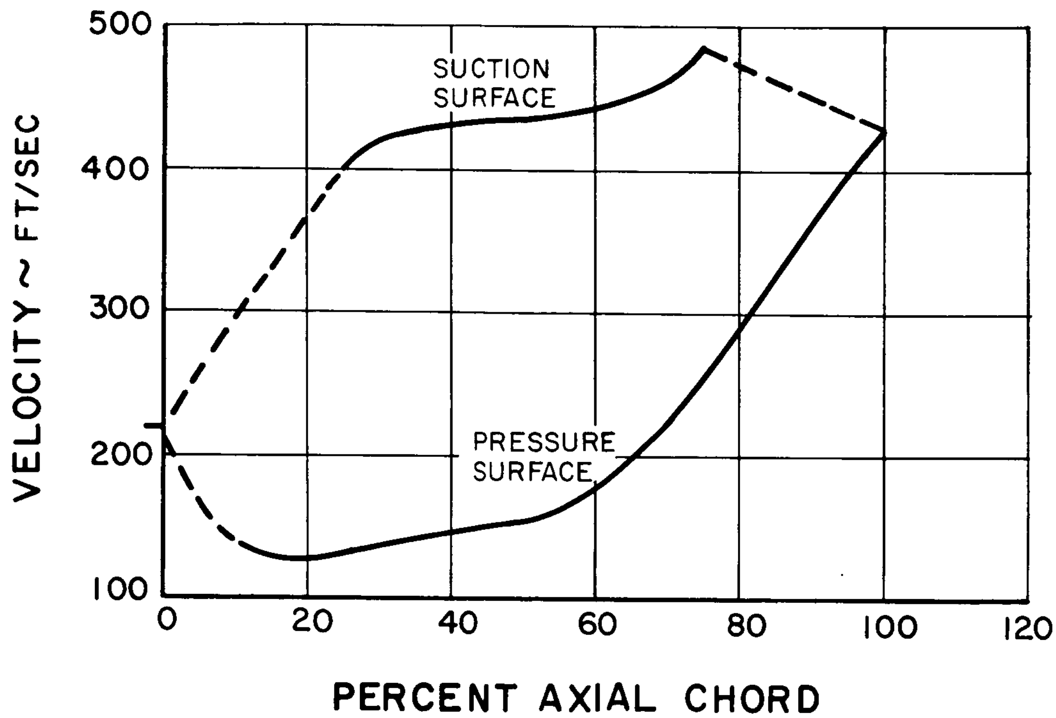

Figure 16 Velocity Distribution at Root Section of Turboalternator Second-Stage Blade

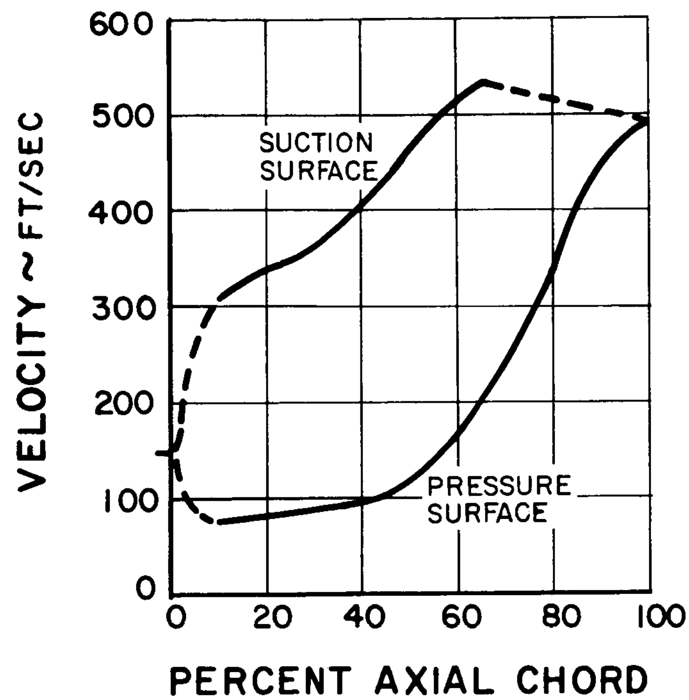

Figure 17 Velocity Distribution at Mean Section of Turboalternator Second-Stage Blade

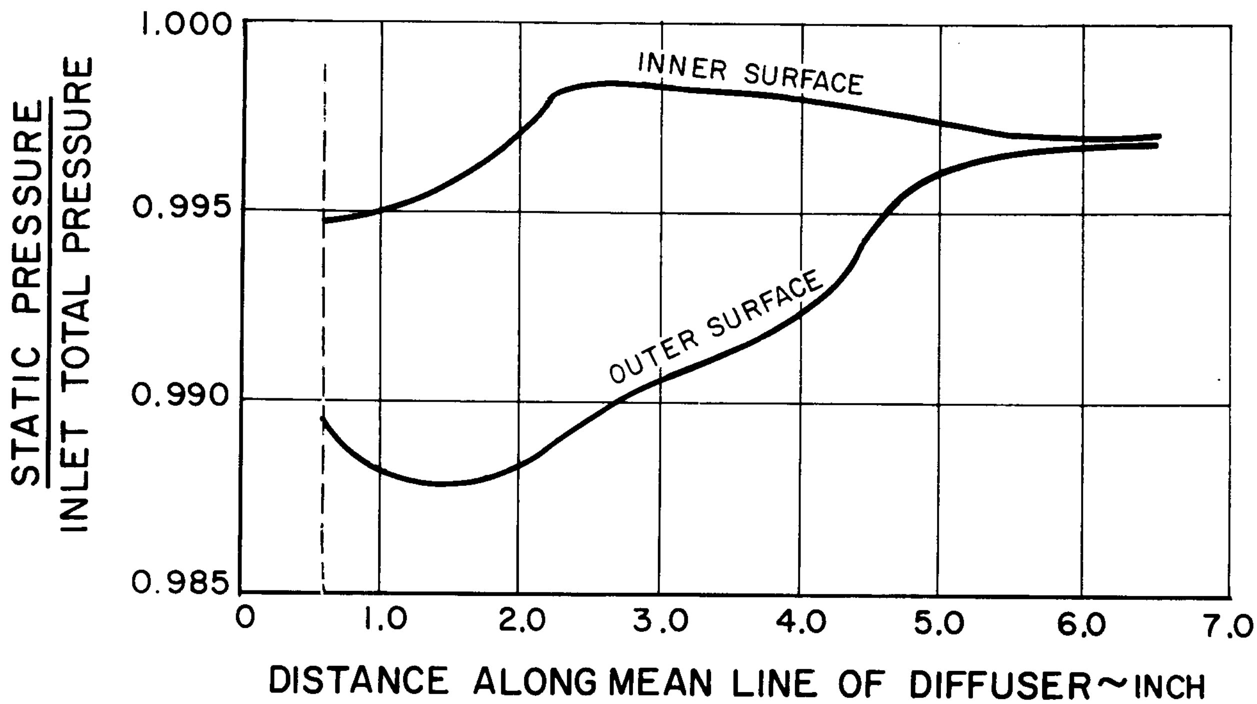

Figure 18 Pressure Distribution in Turbine Exit Diffuser

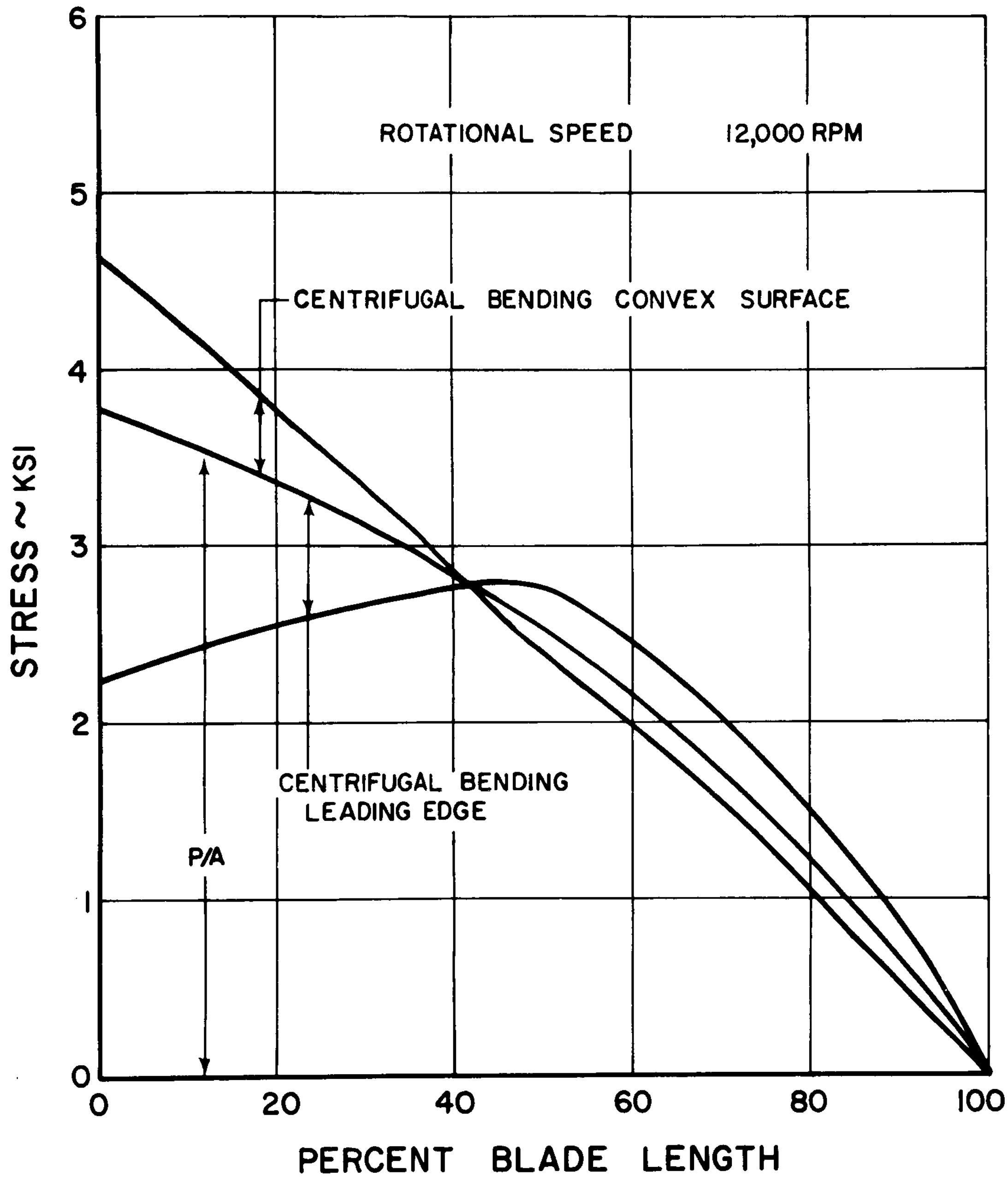

Figure 19 Stress Distribution in Turboalternator First-Stage Blade

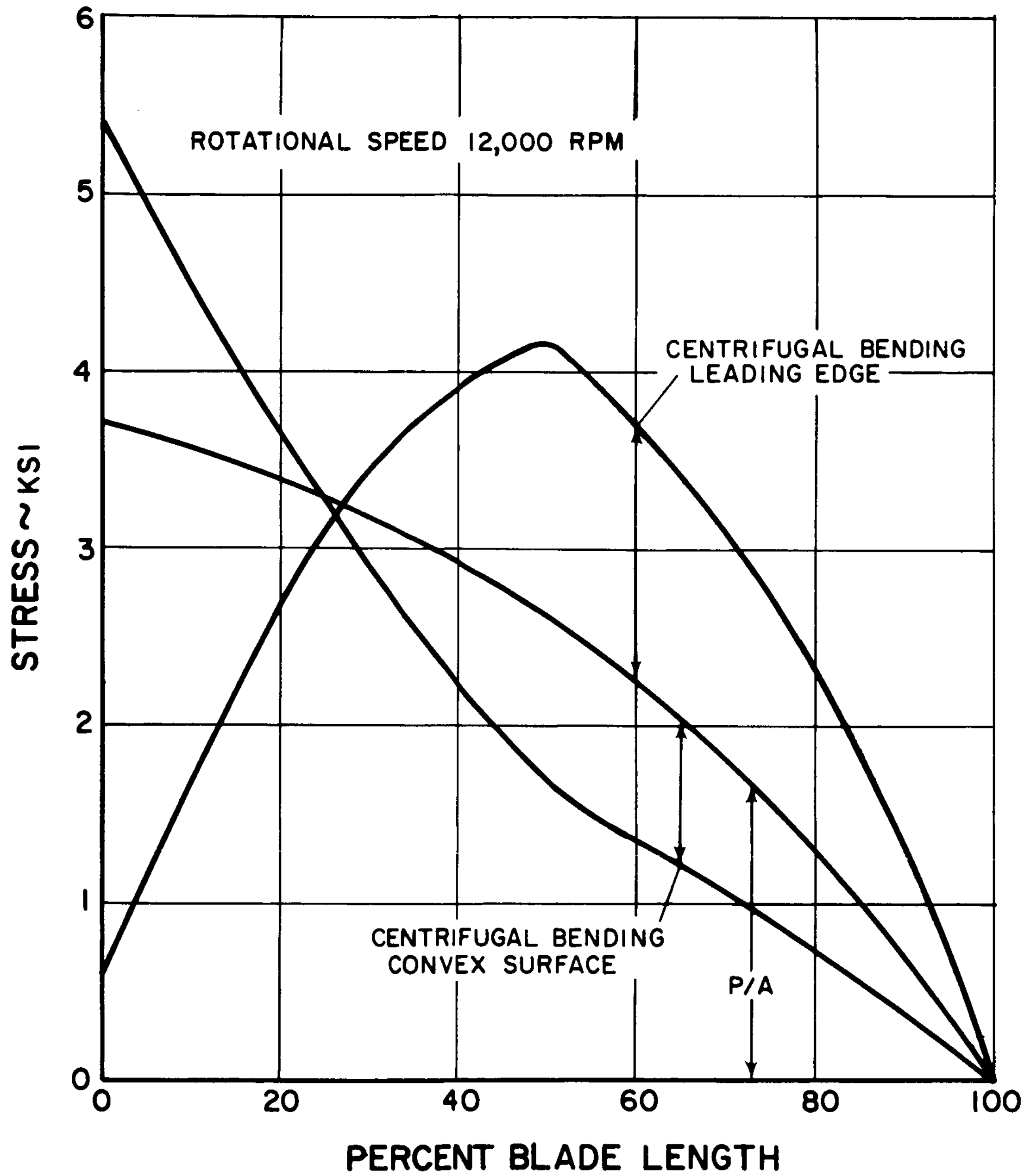

Figure 20 Stress Distribution in Turboalternator Second-Stage Blade

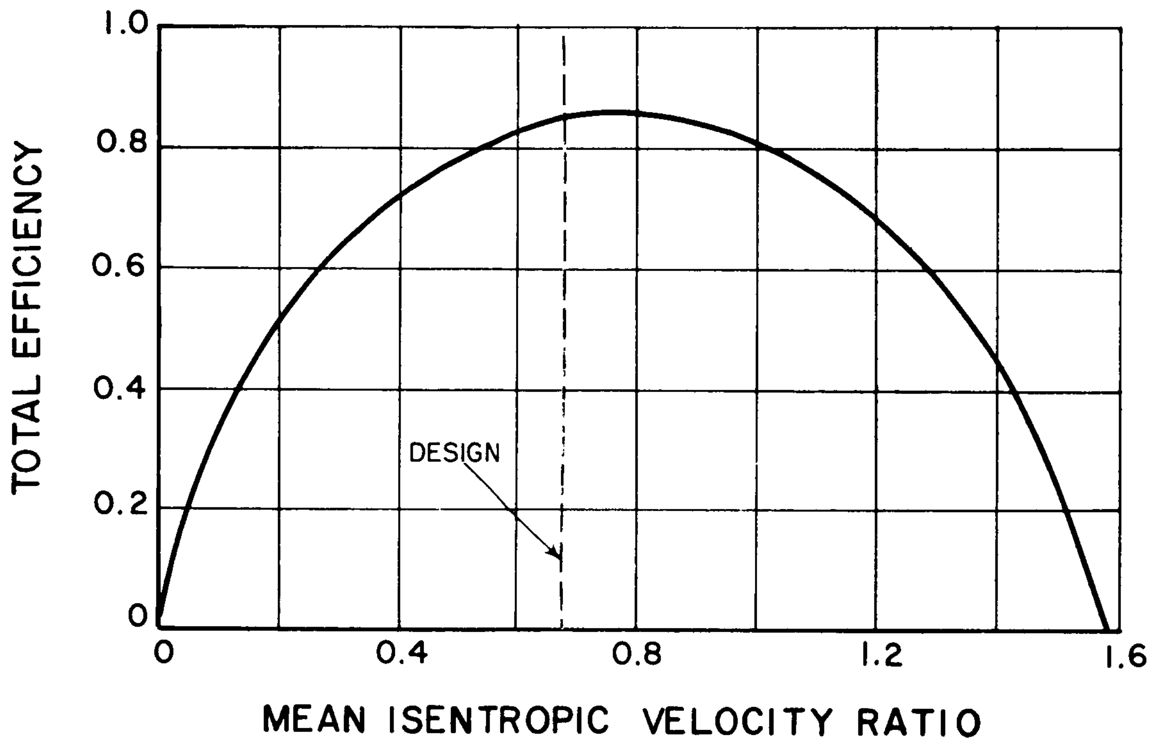

Figure 21 Predicted Performance of the Turbine

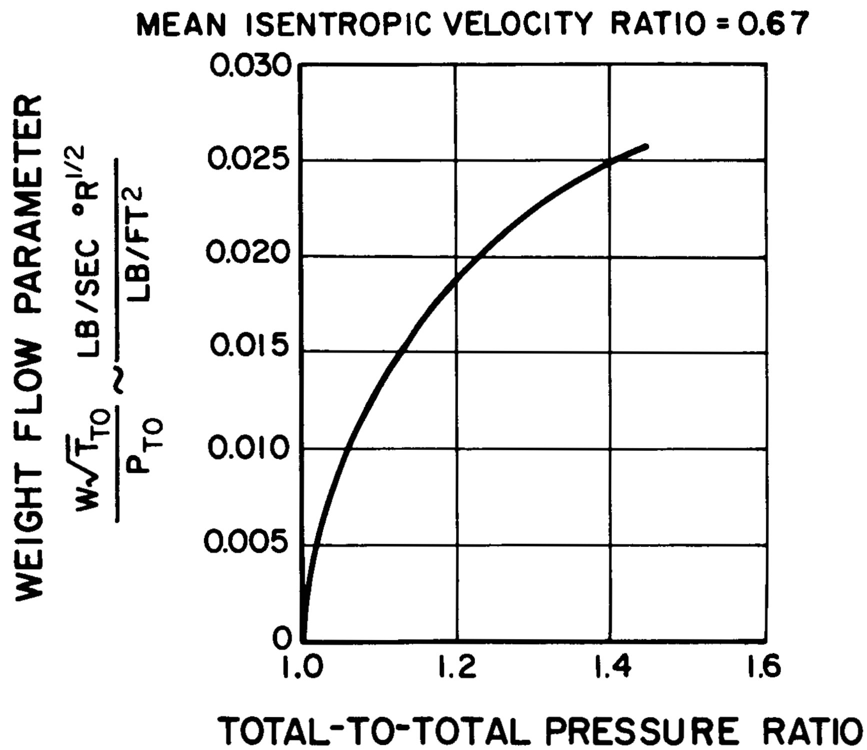

Figure 22 Predicted Weight Flow Parameter for the Turbine

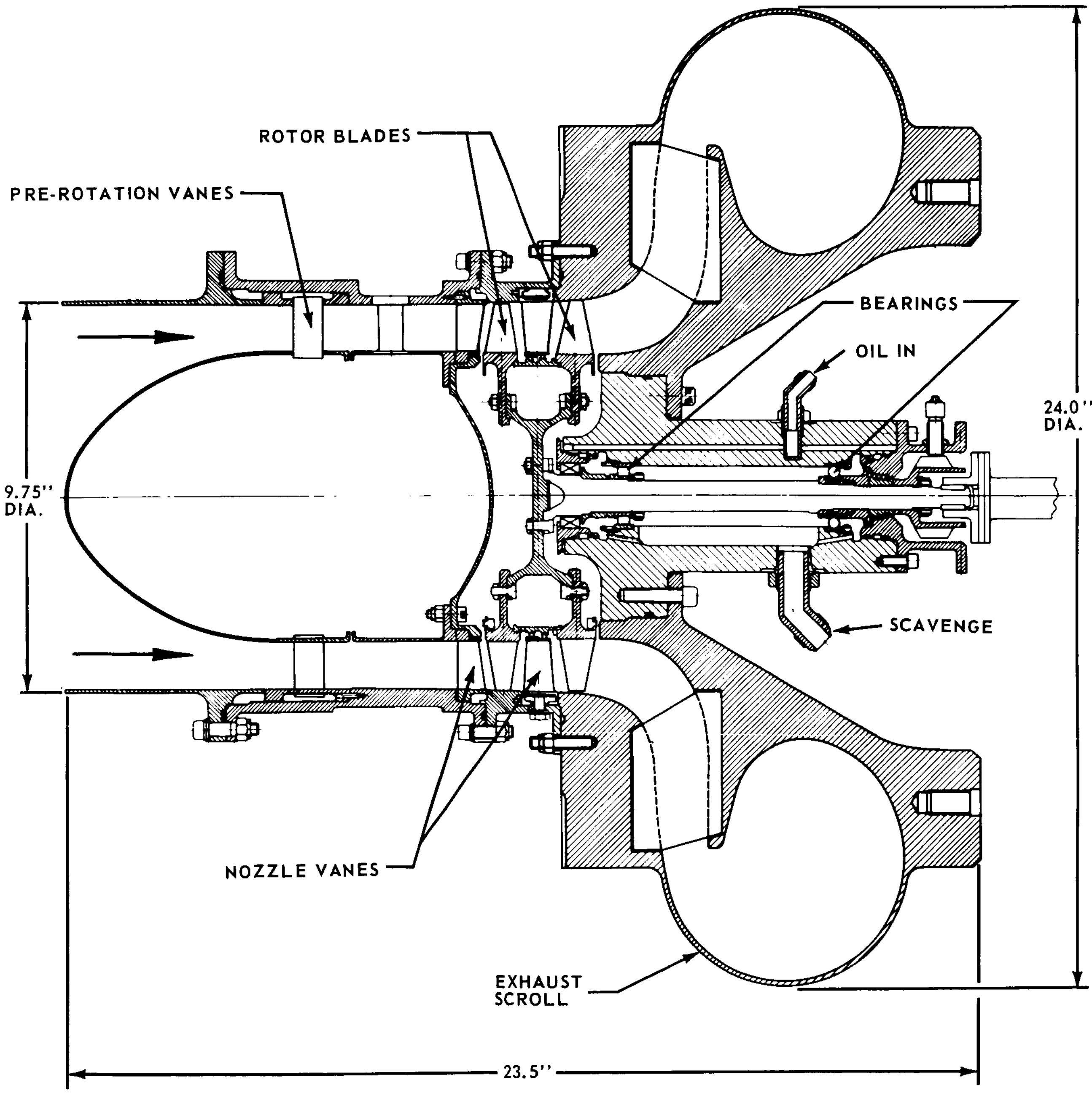

Figure 23 Cross-Section of Turbine Research Package

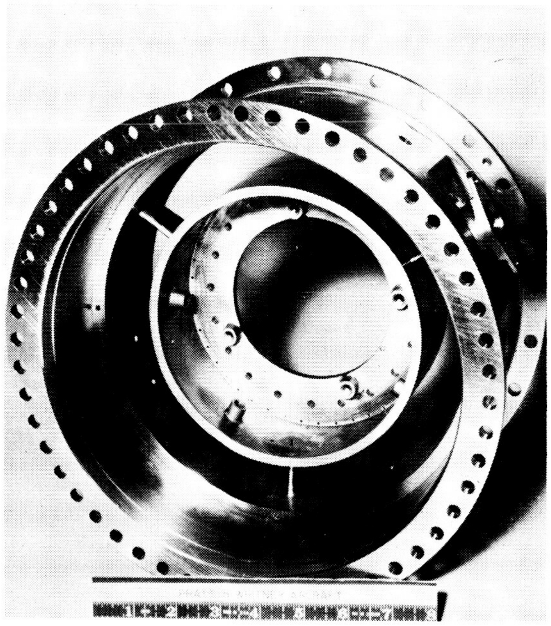

Upstream End View

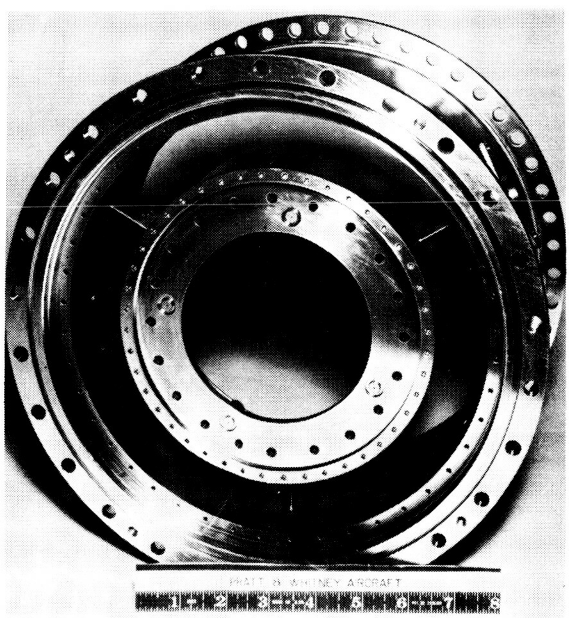

Downstream End View

M-36210

Figure 24 Turbine Inlet Case

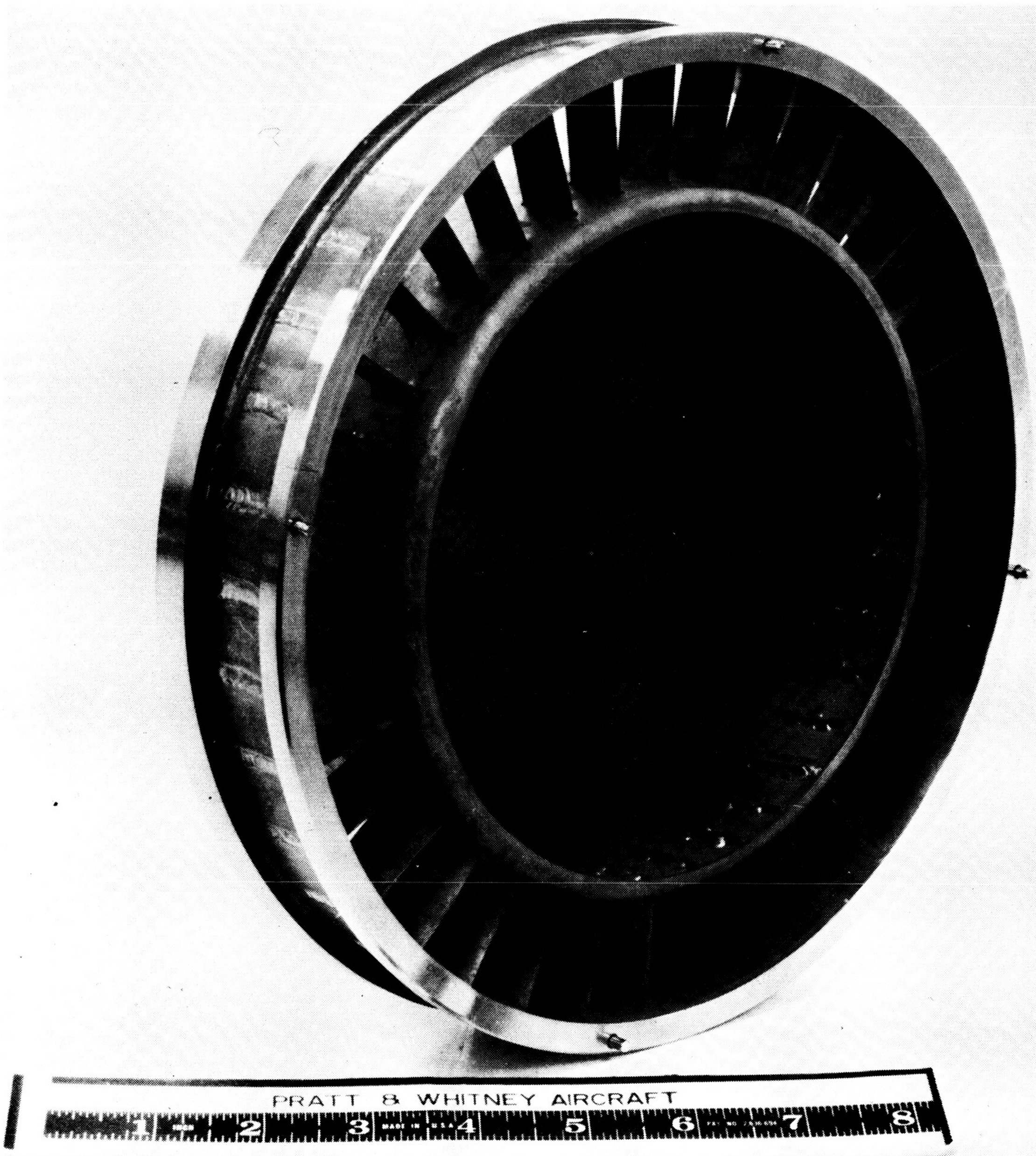

M-36254

Figure 25 Pre-rotation Vane Assembly

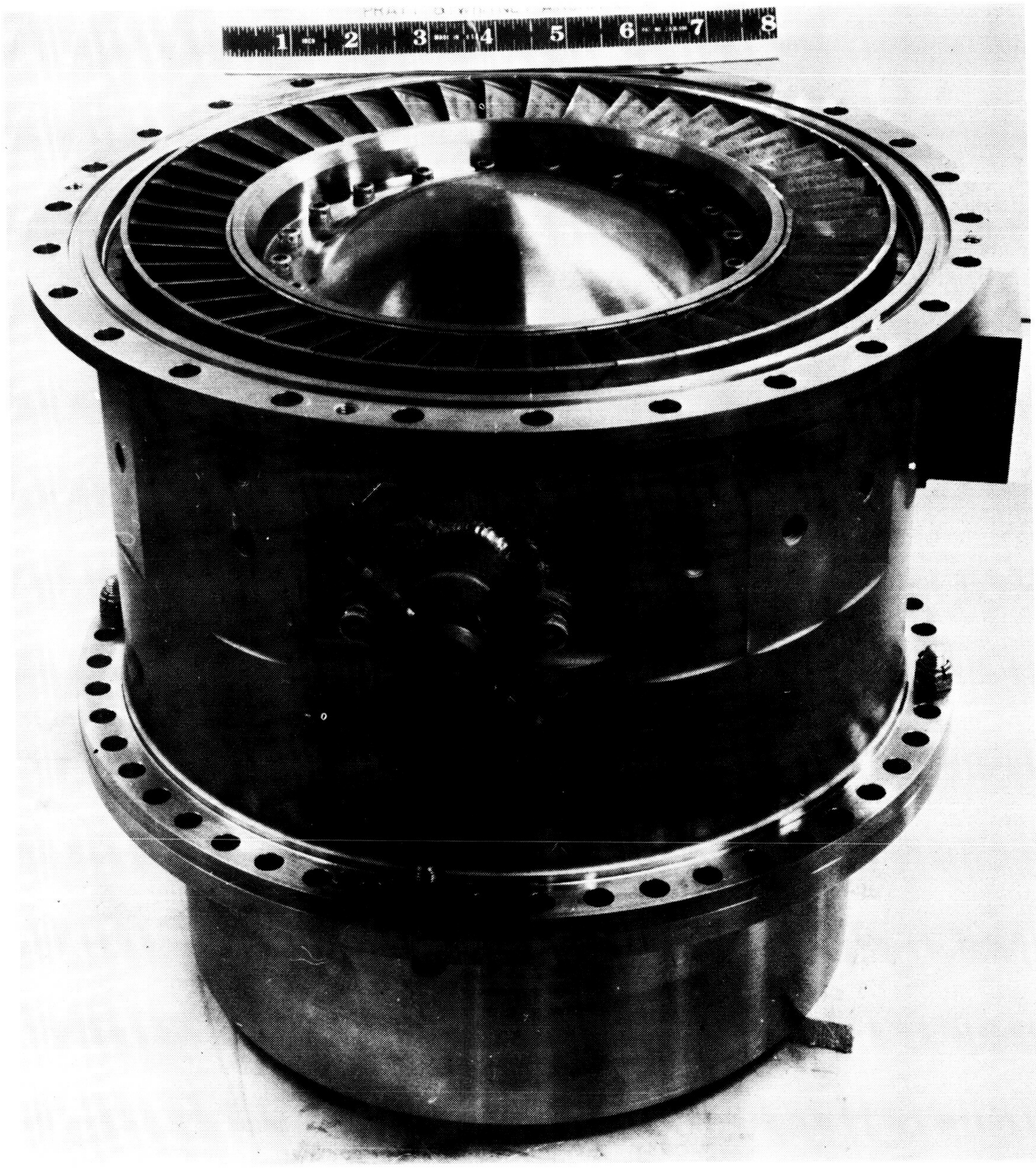

M-36255

Figure 26 Inlet Assembly With First-Stage Nozzle Vanes

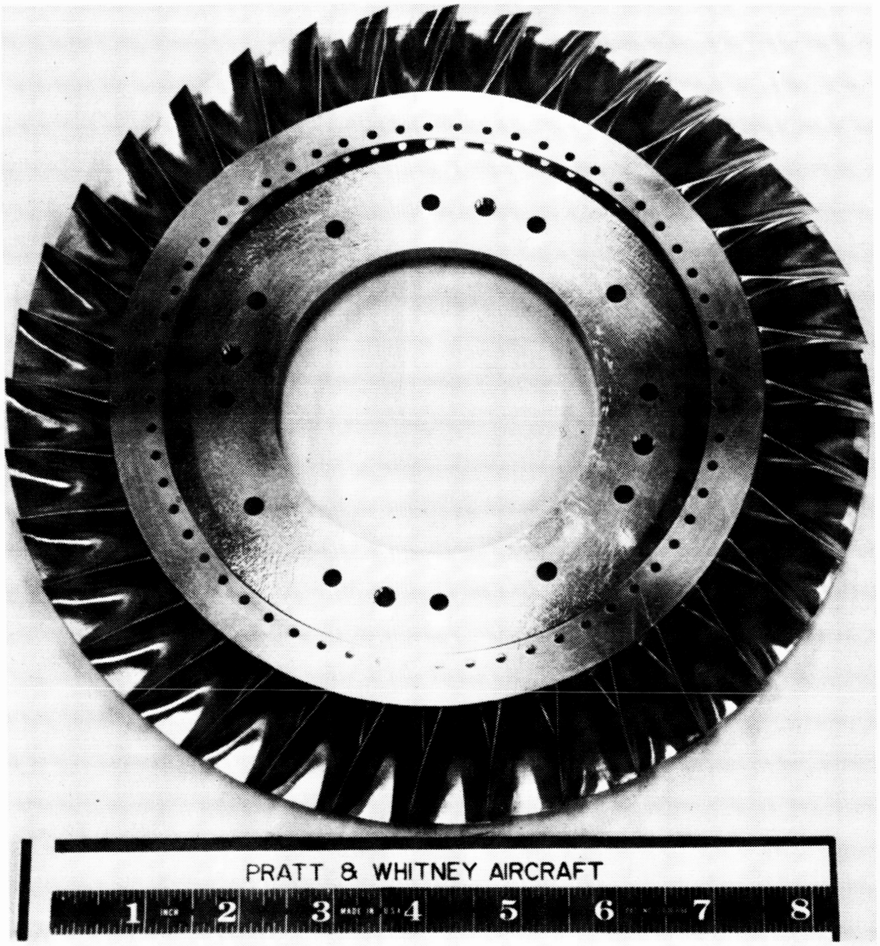

M-36381

Figure 27 First-Stage Wheel

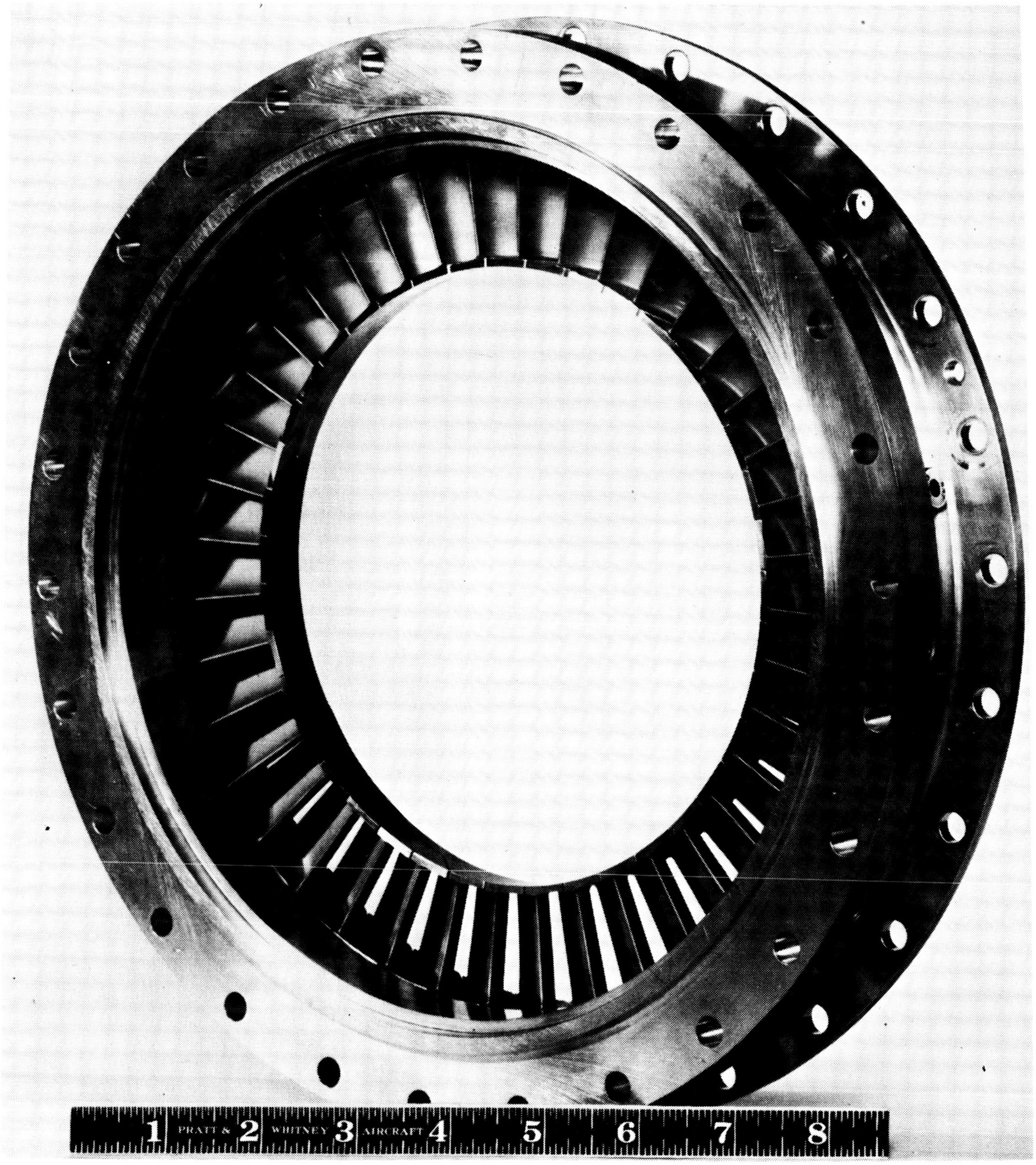

M-36638

Figure 28 Second-Stage Nozzle Assembly

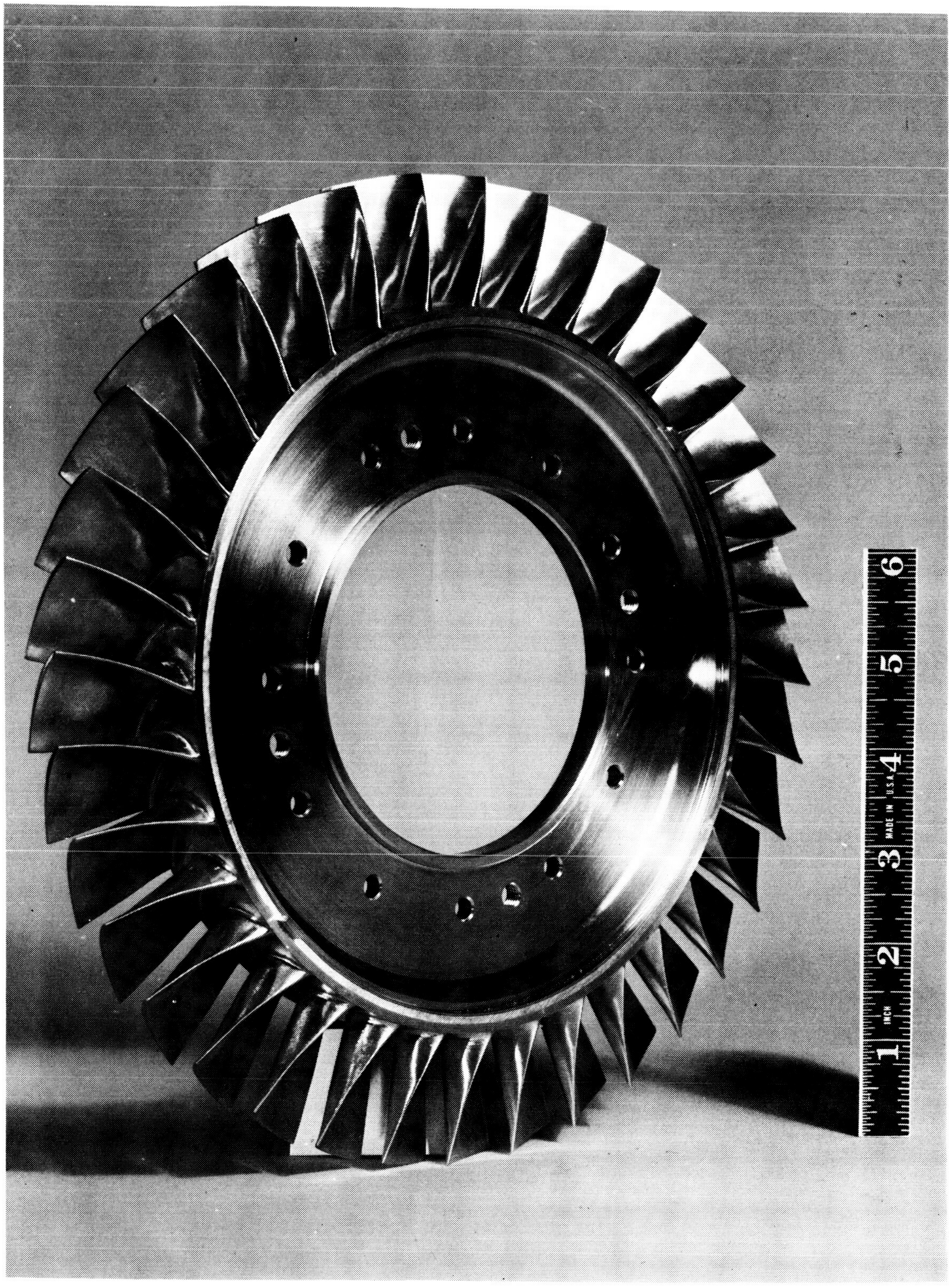

XP-59571

Figure 29 Second-Stage Wheel

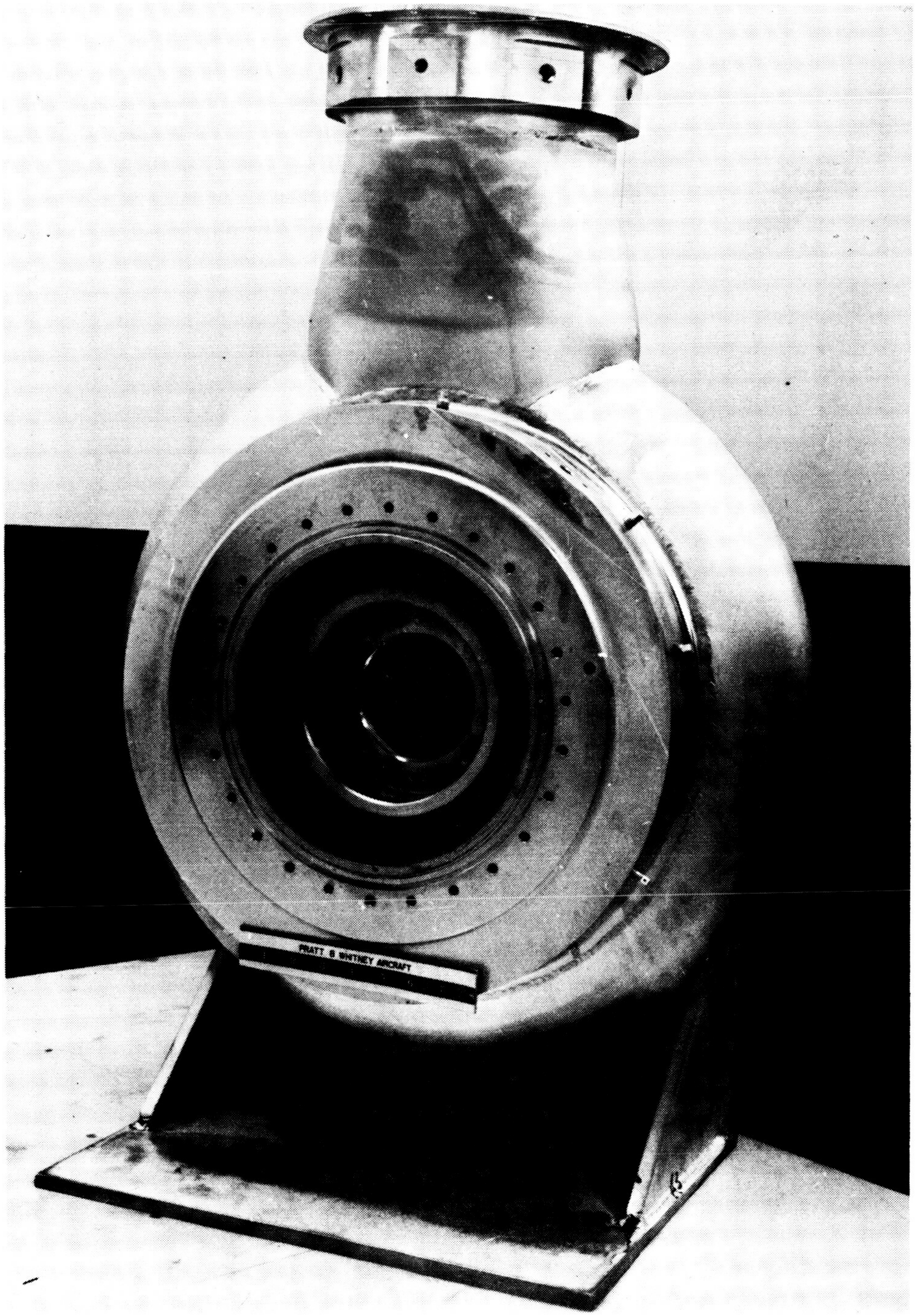

M-36248

Figure 30 Exhaust Scroll

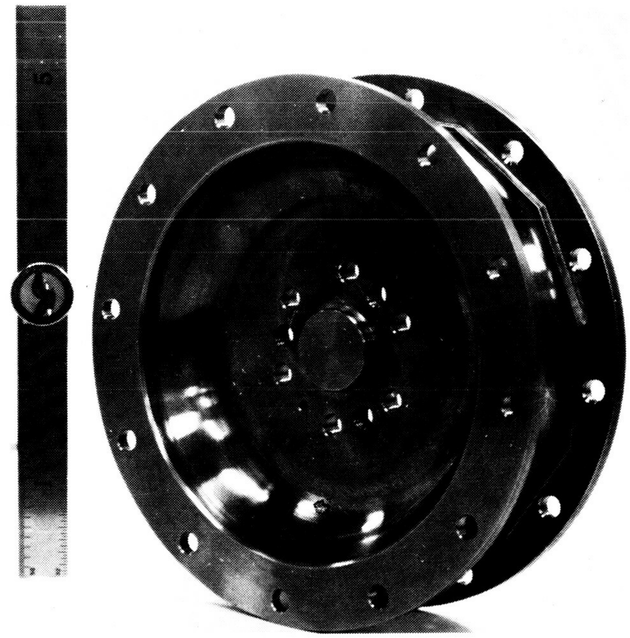

Shaft End

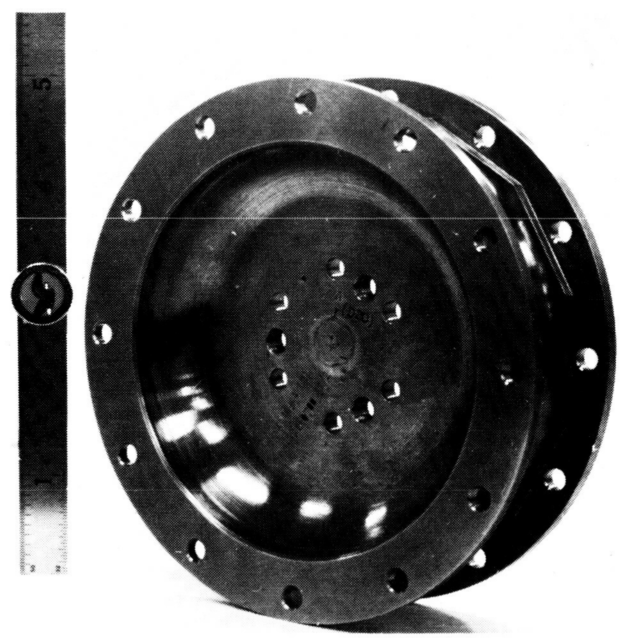

Anti-Shaft End

M-36253

Figure 31 Main Disk

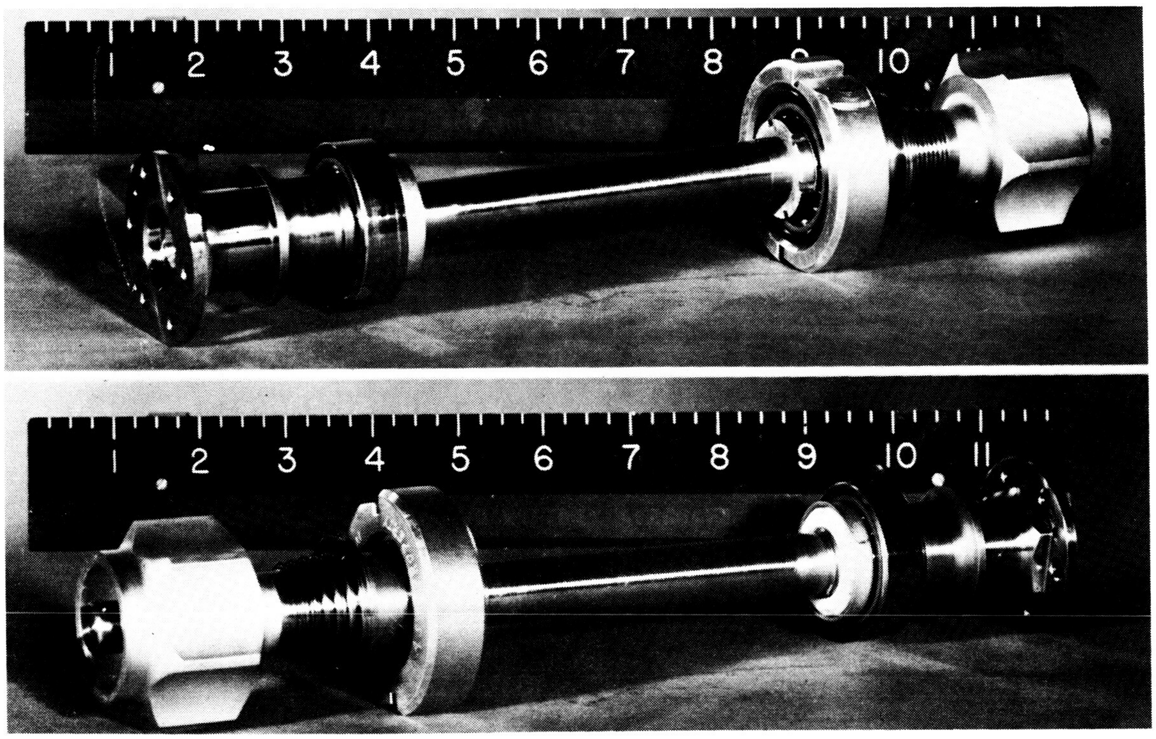

M-36209

Figure 32 Shaft Assembly

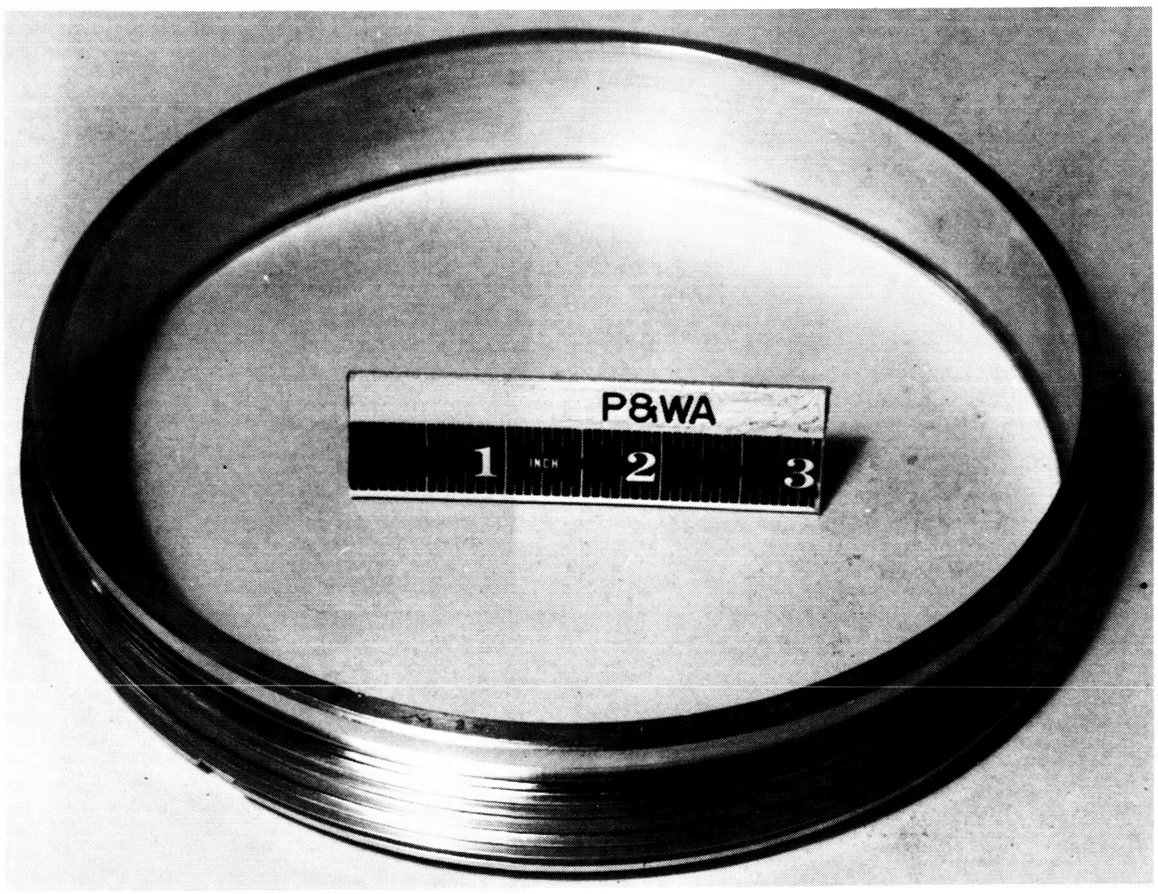

M-36252

Figure 33 Interstage Rotor Seal

M-36251

Figure 34 Bearing Compartment Labyrinth Seal and Speed Pickup Housing

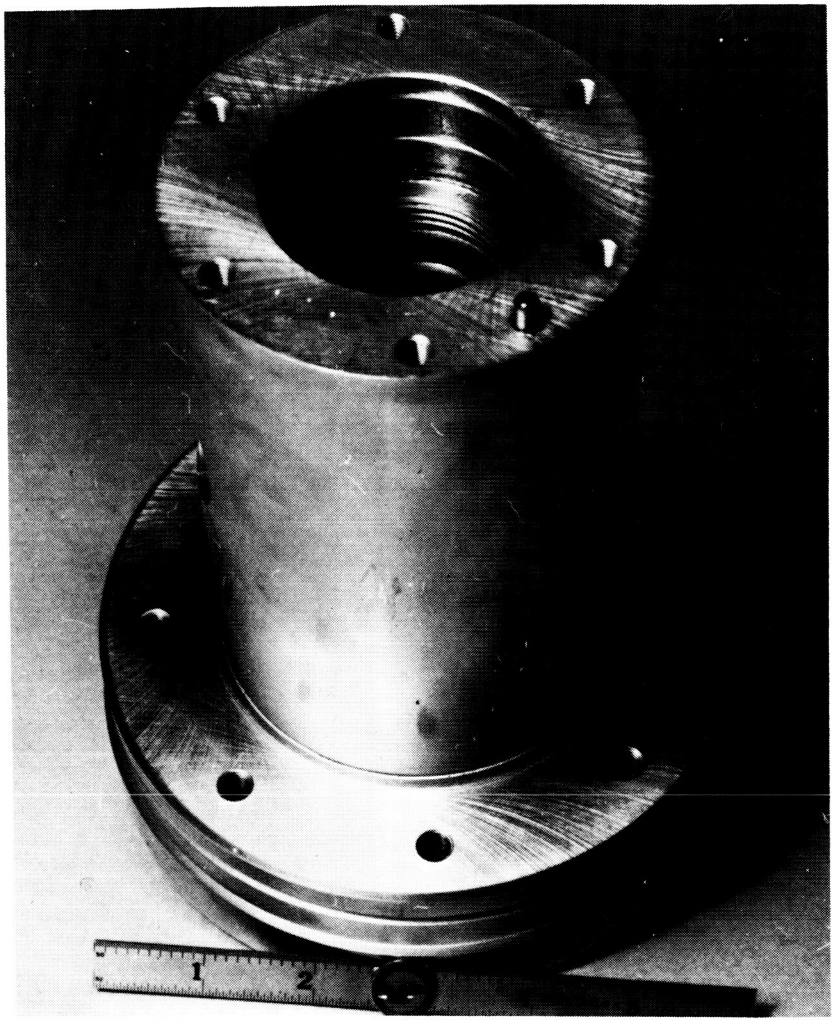

M-36211

Figure 35 Drive End of Main Bearing Housing

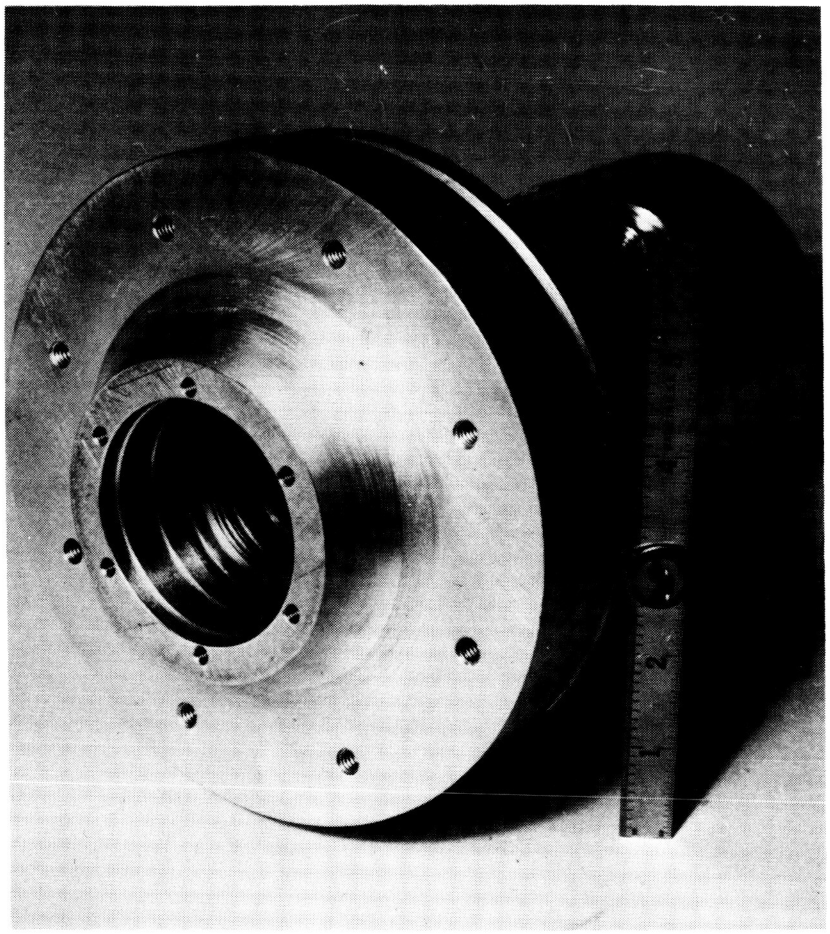

M-36211

Figure 36 Turbine End of Main Bearing Housing

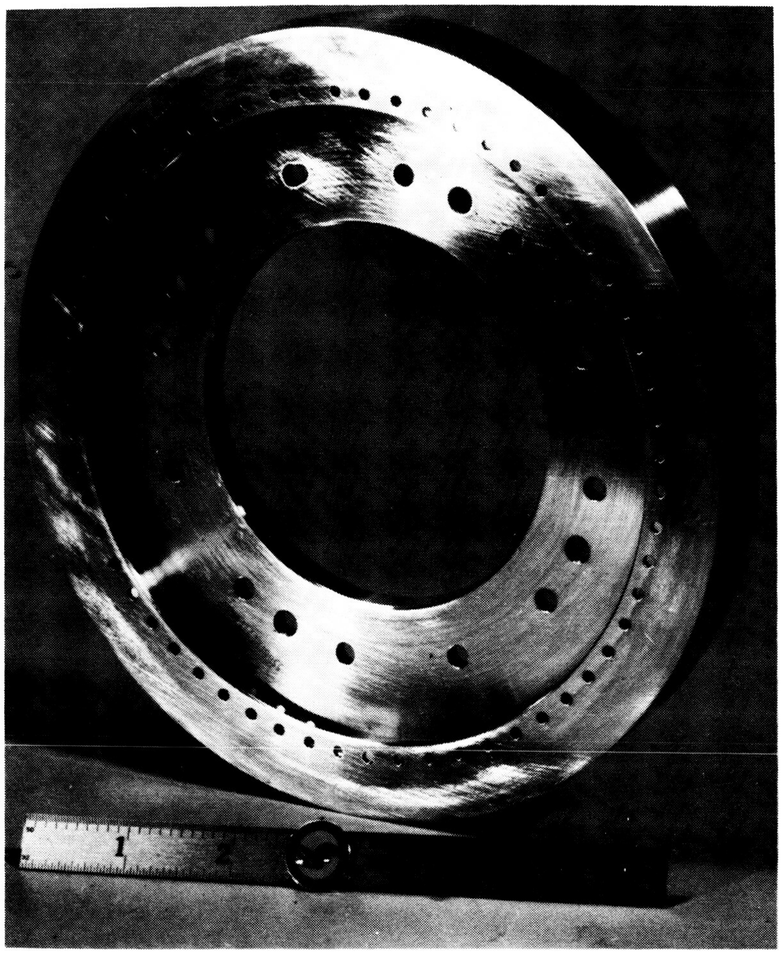

M-36207

Figure 37 Dummy Second-Stage Wheel

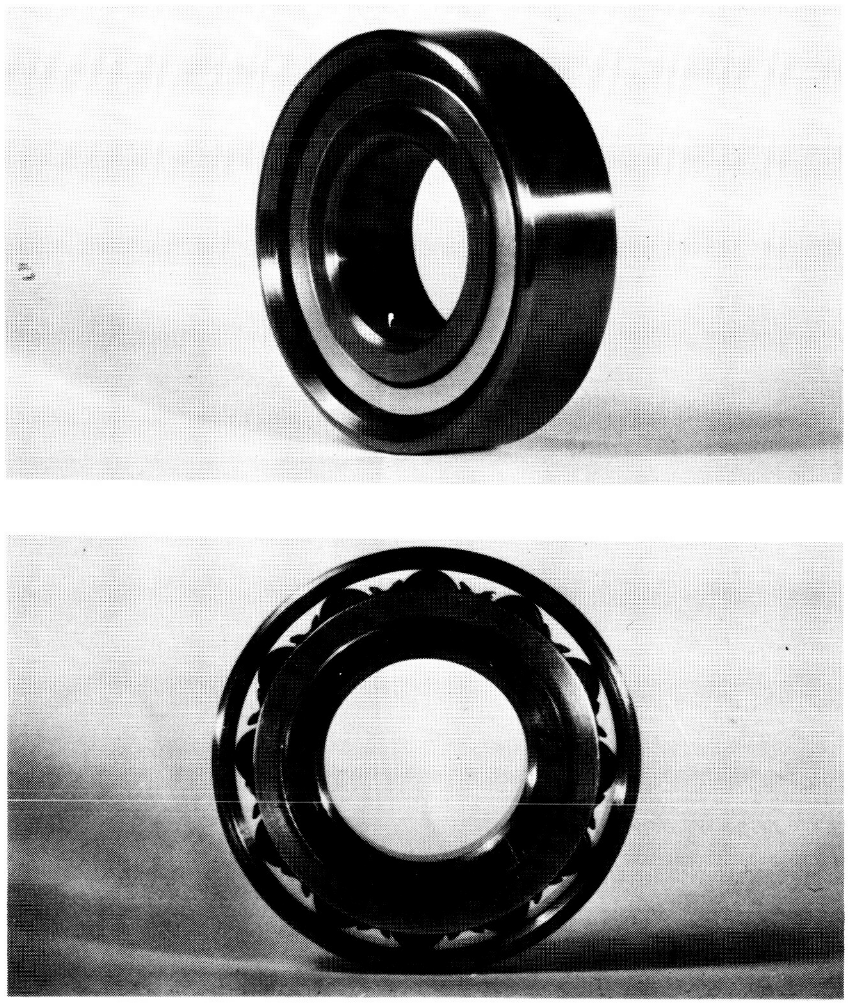

M-37152

Figure 38 Turbine Research Package Roller Bearing

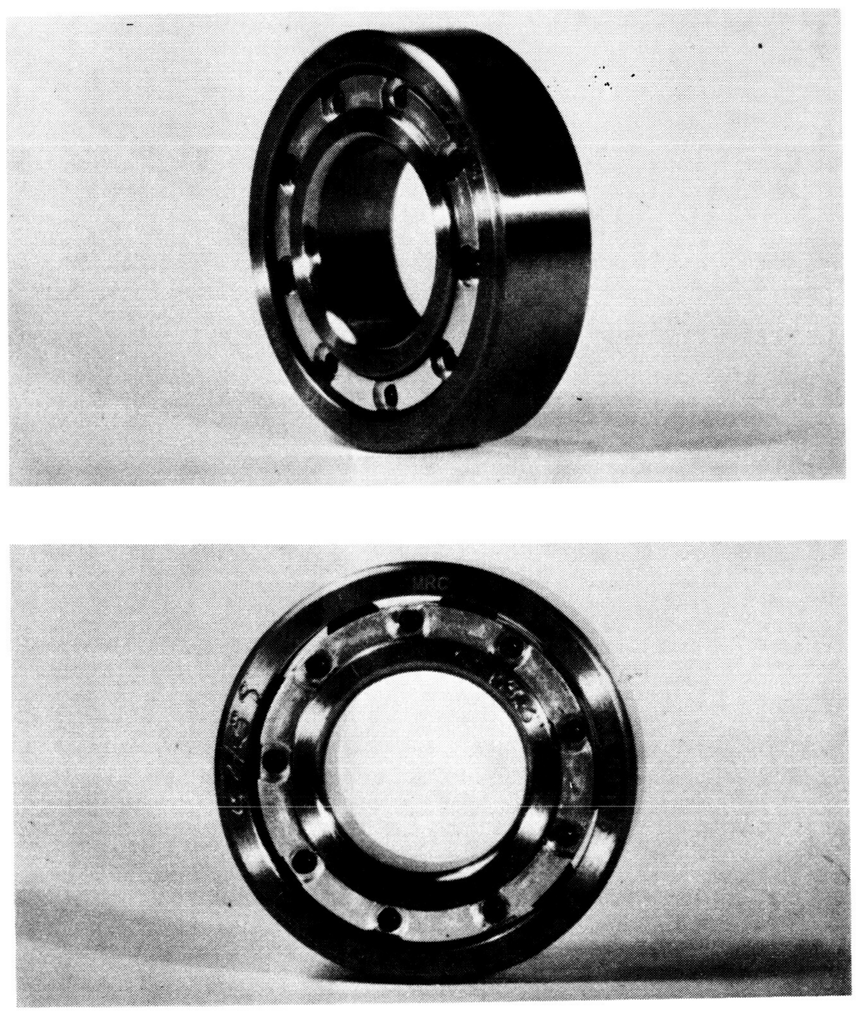

M-37152

Figure 39 Turbine Research Package Ball Bearing

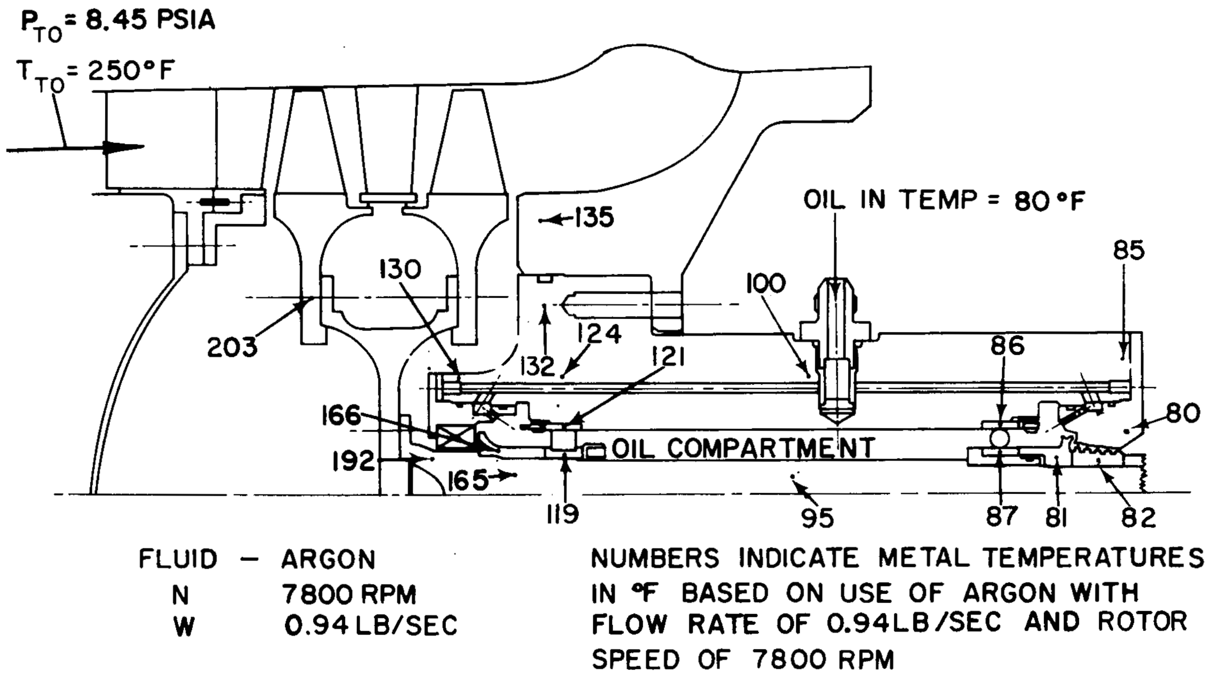

Figure 40 Thermal Map of Turbine Research Package

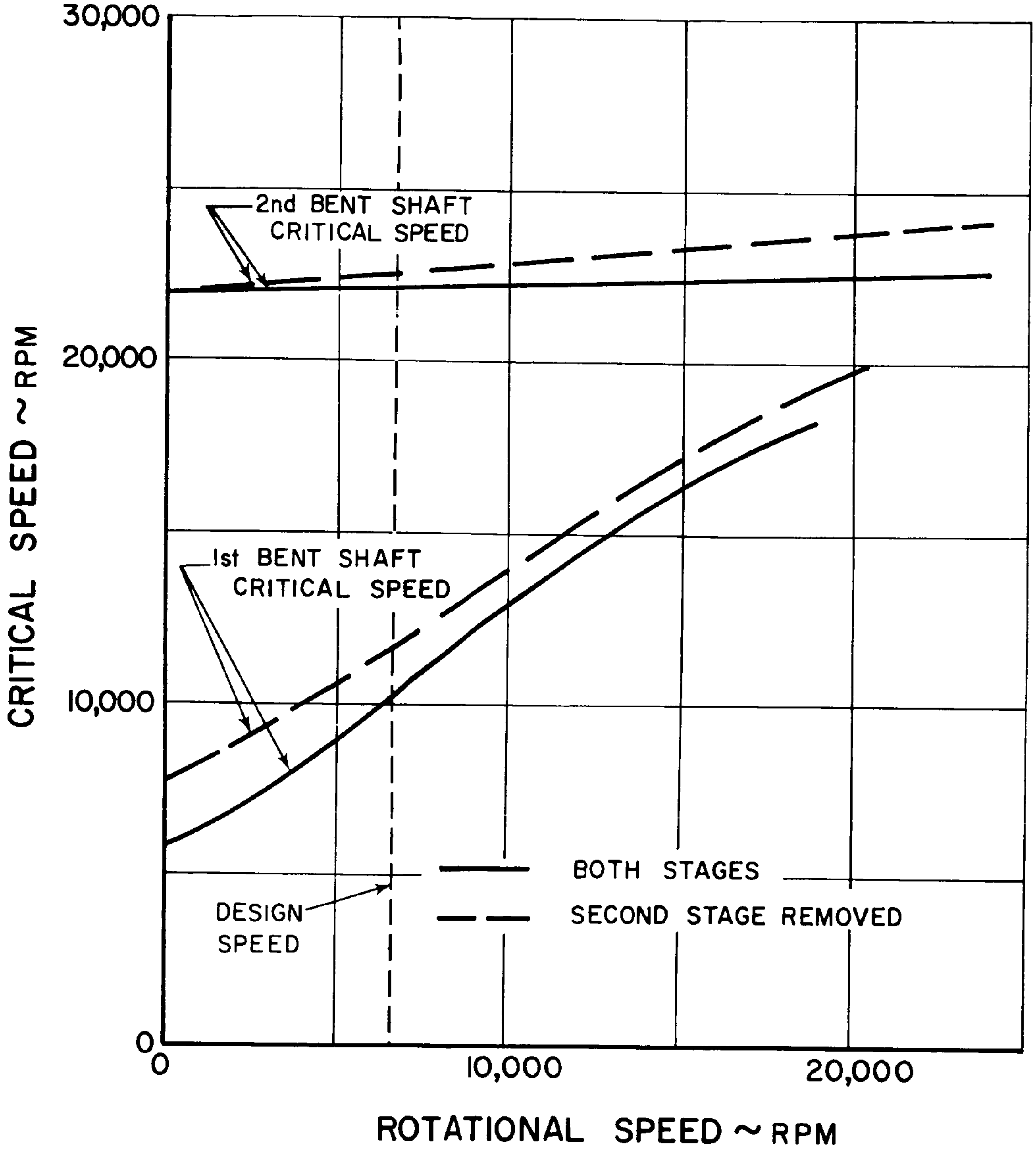

Figure 41 Rotor Critical Speeds

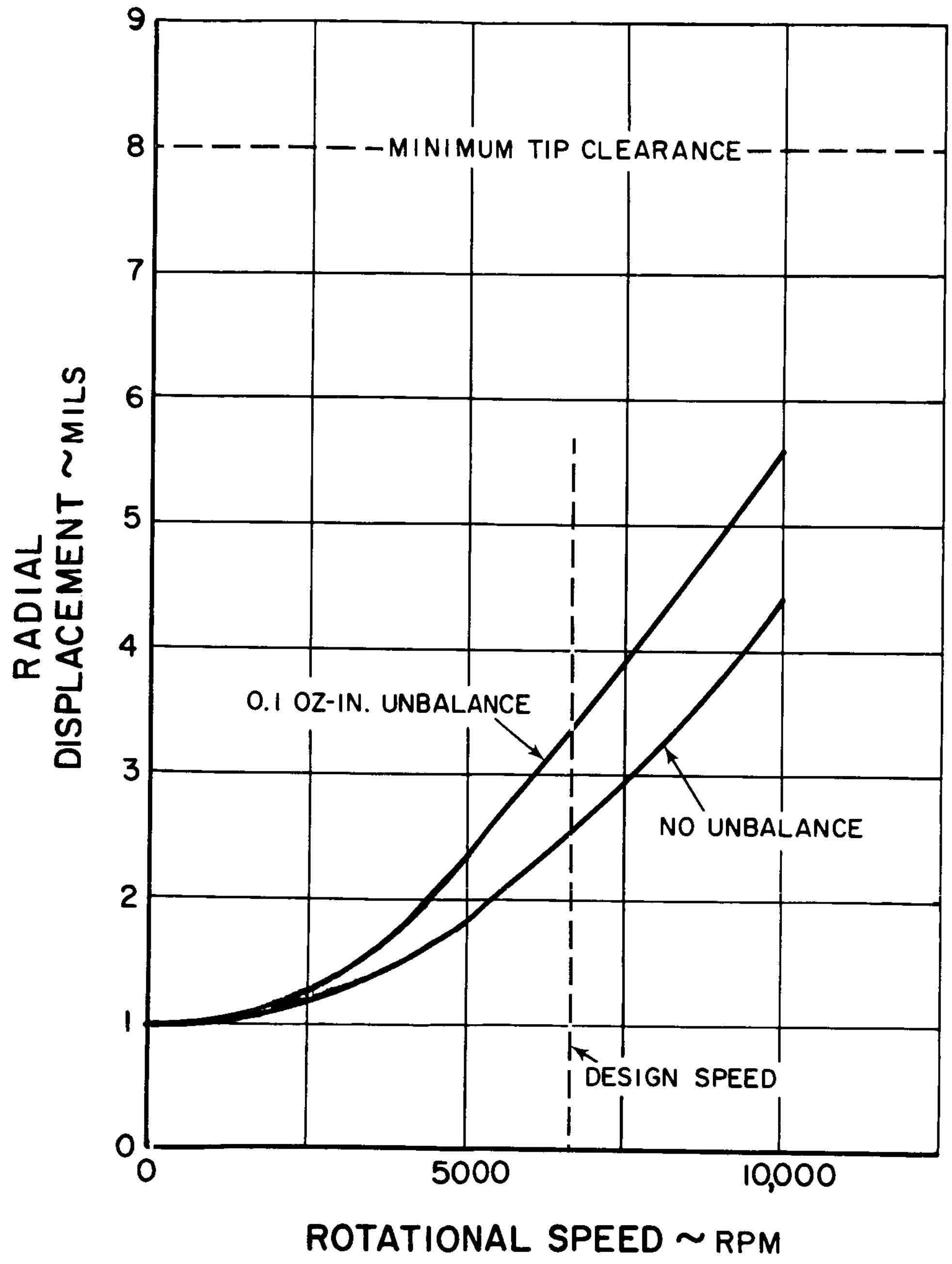

Figure 42 Turbine Wheel Displacement

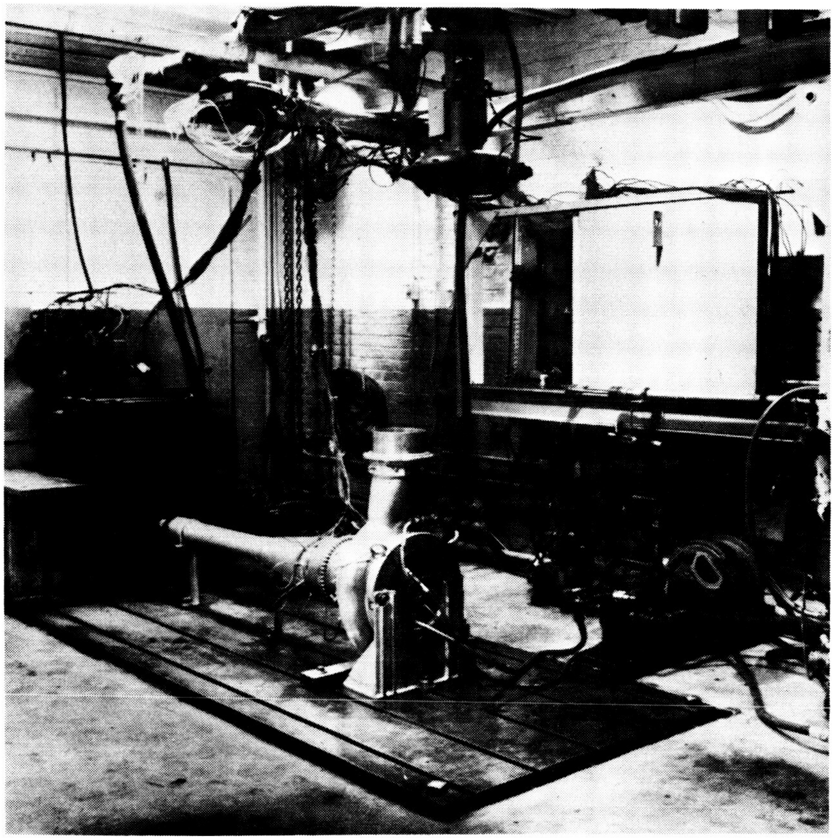

X-21203

Figure 43 - Turbine Research Package Mounted for Acceptance Test

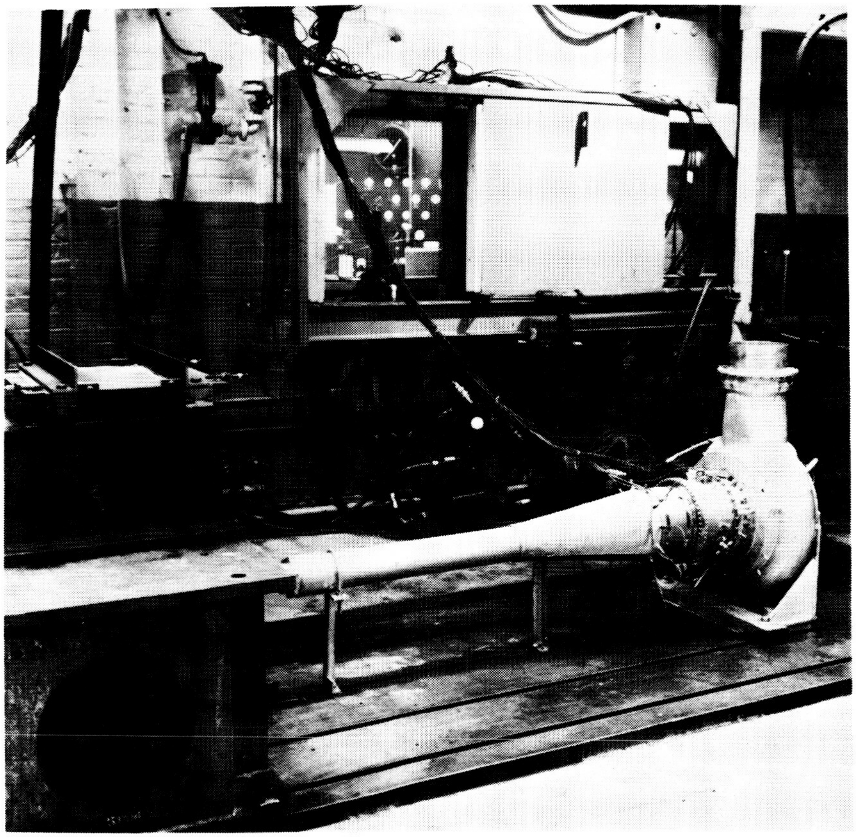

X-21201
Figure 44 - Turbine Research Package Mounted for Acceptance Test

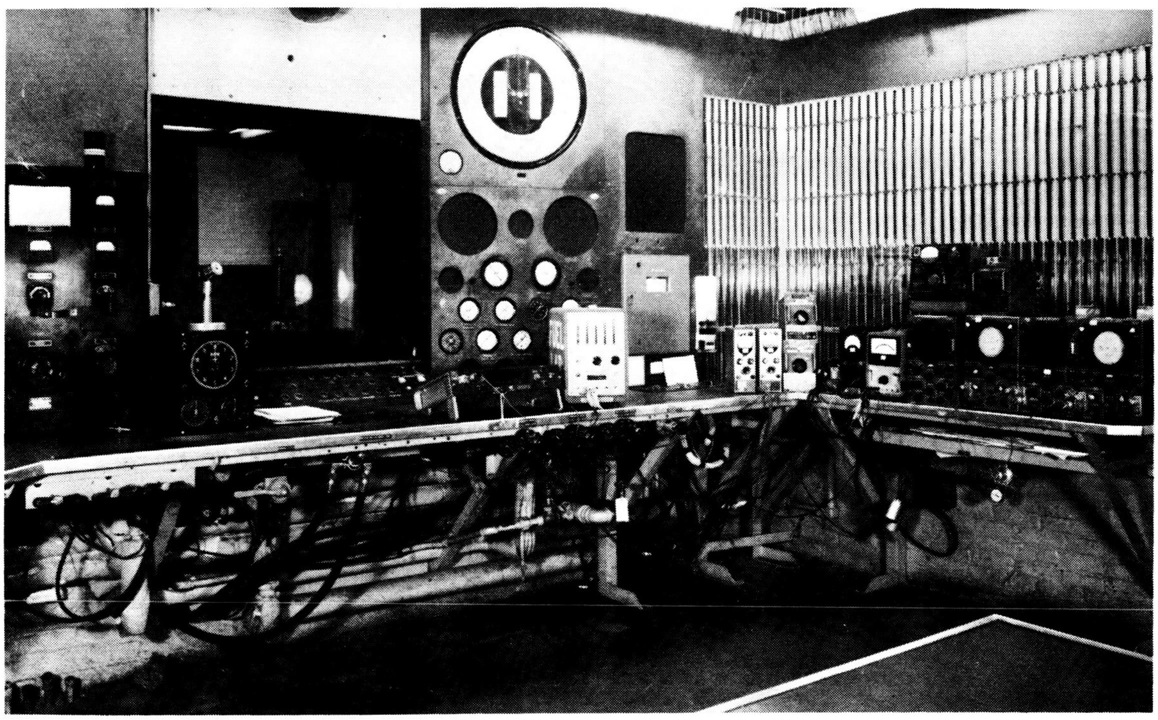

M-37154

Figure 45 - Control Room Used for Turbine Research Package Acceptance Test

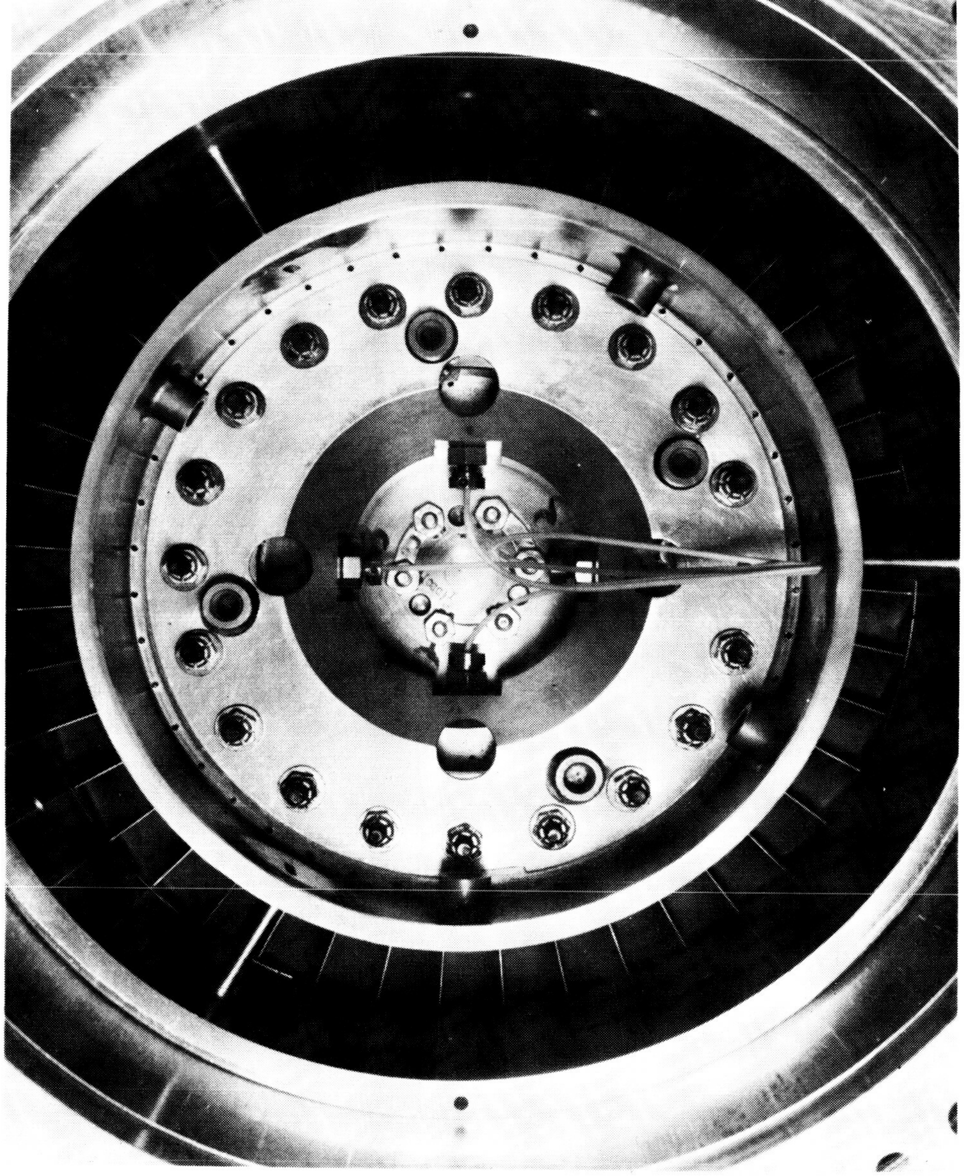

M-37157

Figure 46 - Installation of Proximity Probes

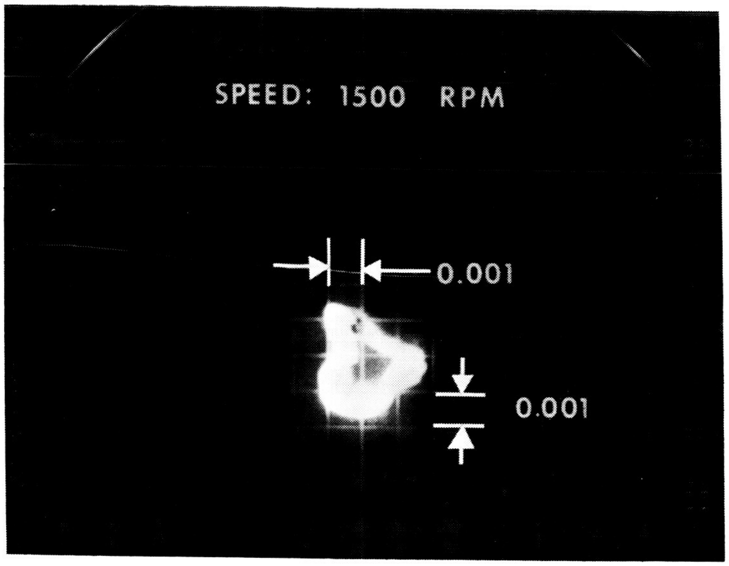

Orbit of First-Stage Disk

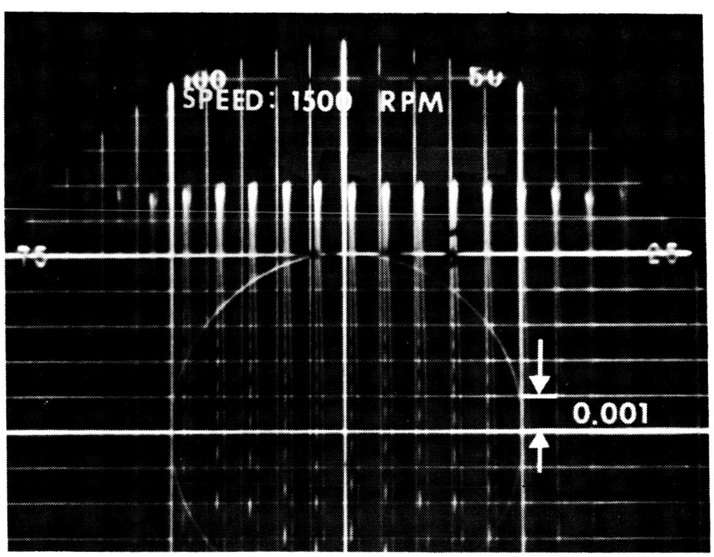

Radial Motion of Six-Tooth Speed Gear

M-37148

Figure 47 - Rotor Dynamic Test Results for Rotor Speed of 1500 RPM

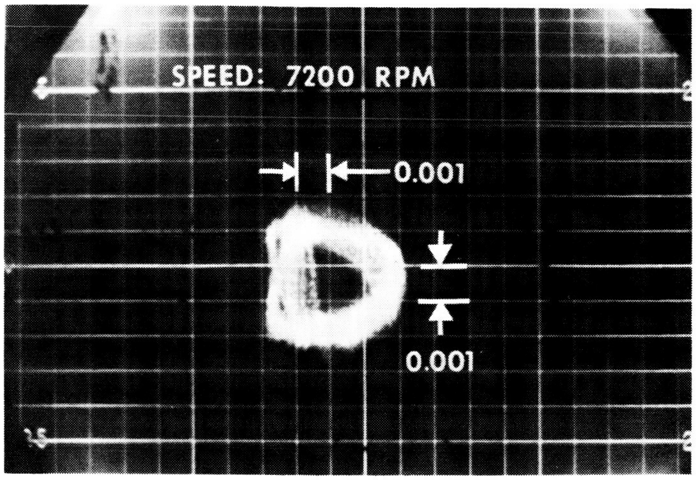

Orbit of First-Stage Disk

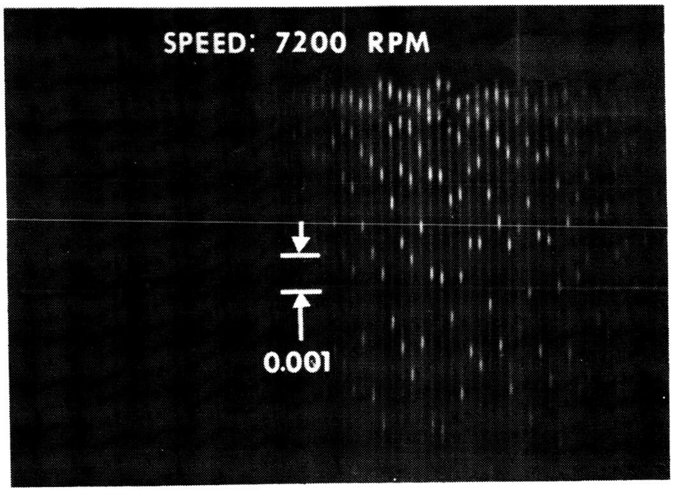

Radial Motion of Six-Tooth Speed Gear

M-37149

Figure 48 Rotor Dynamic Test Results for Rotor Speed of 7200 RPM

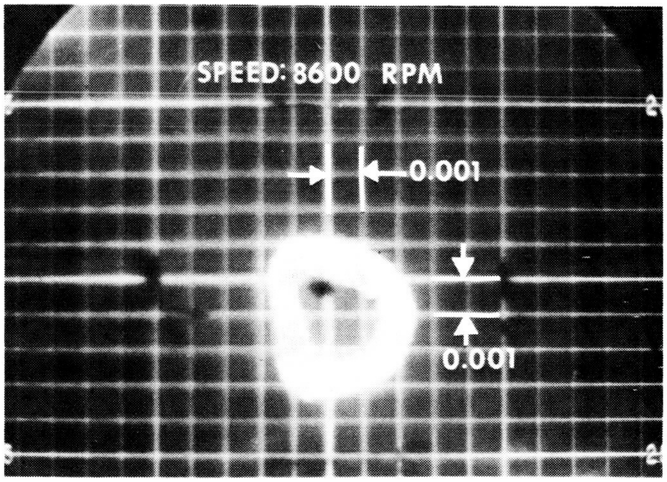

Orbit of First-Stage Disk

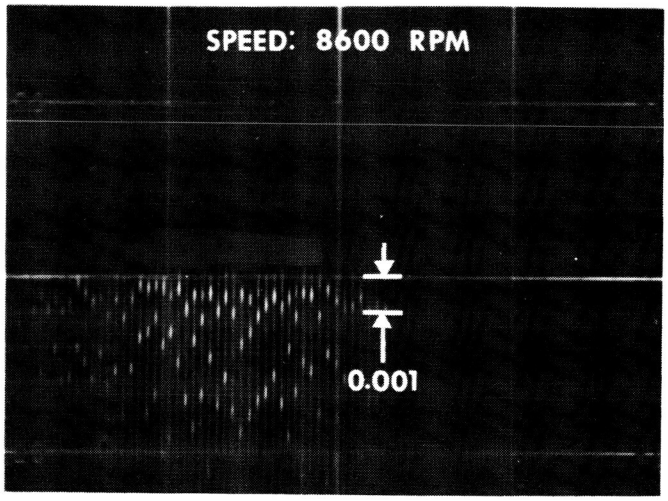

Radial Motion of Six-Tooth Speed Gear

M-37149

Figure 49 Rotor Dynamic Test Results for Rotor Speed of 8600 RPM

APPENDIX

MEASURED TURBINE RESEARCH PACKAGE CLEARANCES

The following clearances were measured during assembly or calculated from measured values in the two-stage version of the turbine research package.

	Clearance (Inch)
First-stage rotor blade radial tip clearance	0.008 to 0.011
Second-stage rotor blade radial tip clearance	0.010 to 0.013
Axial clearance between first-stage nozzle and first-stage rotor	0.237*
Axial clearance between first-stage rotor and second-stage nozzle	0.137*
Axial clearance between second-stage nozzle and second-stage rotor	0.199*
Axial clearance between second-stage rotor and case	0.103*
Interstage labyrinth seal radial clearance	0.016
Interstage labyrinth seal axial clearance	0.096
Drive end labyrinth seal radial clearance	0.010
Total shaft axial play	0.008
Total shaft radial play at hub end	0.003
Total shaft radial play at coupling end	0.0035
Carbon face seal compression	0.077

*Measured at rotor airfoil root

FINAL REPORT
TURBINE RESEARCH PACKAGE FOR RESEARCH AND DEVELOPMENT OF HIGH PERFORMANCE TURBOALTERNATOR

written by

R. Cohen, W. K. Gilroy, F. D. Havens

approved by

P. Bolan

ABSTRACT

The National Aeronautics & Space Administration is conducting an evaluation program of candidate Brayton-cycle turbomachinery configurations. As part of this program, Pratt & Whitney Aircraft is to design, fabricate, and deliver a turboalternator incorporating a two-stage, axial-flow turbine and a 15 KVA, 4-pole inductor alternator supported on gas bearings. A turbine research package is also to be provided to permit evaluation of the aerodynamic performance of the turbine using low-temperature gas. The turbine research package incorporates oil-lubricated, rolling-contact bearings. The aerodynamic and mechanical design of the turbine research package are discussed, and the results of the mechanical tests are presented.

Distribution List
Contract NAS3-6013

National Aeronautics and Space Administration
Washington, D. C. 20546
Attention: Dr. Fred Schulman, RNP — 1
Herbert D. Rochen, RNP — 1
Arvin Smith, RNW — 1

National Aeronautics and Space Administration
Lewis Research Center
21000 Brookpark Road
Cleveland, Ohio 44135
Attention: Jack A. Heller, MS 500-201 — 1
J. E. Dilley, MS 500-309 — 1
J. J. Weber, MS 3-19 — 1
Dr. B. Lubarsky, MS 500-201 — 1
D. G. Beremand, MS 500-201 — 1
J. H. Dunn. MS 500-201 — 1
H. B. Tryon, MS 500-201 — 3
I. I. Pinkel, MS 5-3 — 1
W. L. Stewart, MS 77-2 — 1
H. E. Rohlik, MS 77-2 — 1
M. G. Kofskey, MS 77-2 — 1
D. C. Guentert, MS 500-201 — 1
D. T. Bernatowicz, MS 500-201 — 1
T. A. Moss, MS 500-201 — 1
D. E. Holeski, MS 77-2 — 1
F. J. Dutee, MS 21-4 — 1
R. L. Cummings, MS 500-201 — 1
L. W. Gertsma, MS 500-202 — 1
G. M. Thur, MS 500-201 — 1
R. Y. Wong, MS 77-2 — 1
Report Control Office, MS 5-5 — 1
Reliability & Quality Assurance Office, MS 500-203 — 1
Library, MS 60-3 — 2

NASA Ames Research Center
Moffett Field, California 94035
Attention: Library — 1

NASA Flight Research Center
P.O. Box 273, Edwards, California 93523
Attention: Library — 1

NASA Goddard Space Flight Center
Greenbelt, Maryland 20771
Attention: Library — 1

NASA Langley Research Center
Langley Station, Hampton, Virginia 23365
Attention: Library — 1

NASA Manned Spacecraft Center
Houston, Texas 77058
Attention: Anthony Redding — 1
Library — 1

NASA Marshall Space Flight Center
Huntsville, Alabama 35812
Attention: Library — 1

NASA Western Operations Office
150 Pico Boulevard
Santa Monica, California 90406
Attention: Library — 1

NASA Jet Propulsion Laboratory
4800 Oak Grove Drive
Pasadena, California 91103
Attention: Library — 1

National Aeronautics and Space Administration
Scientific & Technical Information Facility
P.O. Box 33, College Park, Maryland 20740
Attention: Acquisitions Branch, SQT-34054 — 1 + 1 repro

U.S. Army Engineer R&D Laboratories
Gas Turbine Test Facility
Fort Belvoir, Virginia 22060
Attention: W. Crim — 1

Office of Naval Research
Department of the Navy
Washington, D. C. 20025
Attention: Dr. Ralph Roberts — 1

Bureau of Naval Weapons
Department of the Navy
Washington, D. C. 20025
Attention: Code RAPP — 1

Bureau of Ships
Department of the Navy
Washington, D. C. 20025
Attention: G. L. Graves — 1

Air Force Systems Command
Aeronautical Systems Division
Wright-Patterson Air Force Base, Ohio 45433
Attention: Library — 1

Wright-Patterson Air Force Base, Ohio 45433
Attention: John L. Morris, APFL — 1
George Thompson, APFL — 1

Institute for Defense Analyses
400 Army - Navy Drive
Arlington, Virginia 22202
Attention: Library — 1

University of Pennsylvania
Power Information Center
Moore School Building
200 South 33rd Street
Philadelphia, Pennsylvania 19104 — 1

Massachusetts Institute of Technology
Cambridge, Massachusetts 02139
Attention: Library — 1

Aerojet General Corporation
Azusa, California 91703
Attention: Library — 1

AiResearch Manufacturing Company
The Garrett Corporation
402 South 36th Street
Phoenix, Arizona 85034
Attention: Hugh H. Milligan — 1
Library — 1

AiResearch Manufacturing Company
The Garrett Corporation
9851 Sepulveda Boulevard
Los Angeles, California 90009
Attention: Library — 1

Bendix Research Laboratories Division
Southfield (Detroit), Michigan 48232
Attention: Library — 1

The Boeing Company
Aero-Space Division
Box 3707
Seattle, Washington 98124
Attention: Library 1

Borg-Warner Corporation
Pesco Products Division
24700 North Miles Road
Bedford, Ohio 44014
Attention: Library 1

Continental Aviation & Engineering Corporation
12700 Kercheval Avenue
Detroit, Michigan 48215
Attention: Library 1

Curtiss-Wright Corporation
Wright Aero Division
Main and Passaic Streets
Woodridge, New Jersey 07075
Attention: Library 1

Douglas Aircraft Company
3000 Ocean Park Boulevard
Santa Monica, California 90406
Attention: Library 1

General Dynamics Corporation
16501 Brookpark Road
Cleveland, Ohio 44142
Attention: Library 1

General Electric Company
Flight Propulsion Laboratory Division
Cincinnati, Ohio 45215
Attention: Library 1

General Electric Company
Lynn, Massachusetts 01905
Attention: Library 1

General Electric Company
Missile & Space Vehicle Department
3198 Chestnut Street
Philadelphia, Pennsylvania 19104
Attention: Library 1

General Motors Corporation
Indianapolis, Indiana 46206
Attention: Library 1

Lear Siegler, Inc.
3171 S. Bundy Drive
Santa Monica, California 90406
Attention: Library 1

Lockheed Missiles & Space Company
P.O. Box 504
Sunnyvale, California 94088
Attention: Library 1

Mechanical Technology Incorporated
968 Albany-Shaker Road
Latham, New York 12110
Attention: Library 2

North American Aviation, Inc.
Space and Information Systems Division
Downey, California 90241
Attention: Library 1

Northern Research & Engineering Company
219 Vassar Street
Cambridge, Massachusetts 02139
Attention: Library 1

Solar Division of International Harvester
2200 Pacific Highway
San Diego, California 92112
Attention: Library 1

Space Technology Laboratories, Inc.
One Space Park
Redondo Beach, California 90278
Attention: Library 1

Sunstrand Denver
2480 West 70th Avenue
Denver, Colorado 80221
Attention: Library 1

Thompson-Ramo-Wooldridge Accessories Division
23555 Euclid Avenue
Cleveland, Ohio 44117
Attention: Library 1

Union Carbide Corporation
Linde Division
P.O. Box 44, Tonawanda, New York 14152
Attention: Library 1

United Aircraft Research Laboratory
East Hartford, Connecticut 06108
Attention: Library 1

Westinghouse Electric Corporation
Astronuclear Laboratory
P.O. Box 10864, Pittsburgh, Pennsylvania 15236
Attention: Library 1

Williams Research
Walled Lake, Michigan 48088
Attention: Library 1